GLOBAL BIOGEOCHEMICAL CYCLES, VOL. 11, NO. 2, PAGES 235-266, JUNE 1997

Global patterns of marine nitrogen fixation and denitrification

Nicolas Gruber

Climate and Environmental Physics, Physics Institute, University of Bern, Bern, Switzerland

Jorge L. Sarmiento

Program in Atmospheric and Oceanic Sciences, Princeton University, Princeton, New Jersey

Abstract. A new quasi-conservative tracer N^*, defined as a linear combination of nitrate and phosphate, is proposed to investigate the distribution of nitrogen fixation and denitrification in the world oceans. Spatial patterns of N^* are determined in the different ocean basins using data from the Geochemical Ocean Sections Study (GEOSECS) cruises (1972-1978) and from eight additional cruises in the Atlantic Ocean. N^* is low (< -3 μmol kg^{-1}) in the Arabian Sea and in the eastern tropical North and South Pacific. This distribution is consistent with direct observations of water column denitrification in these oxygen minimum zones. Low N^* concentrations in the Bering Sea and near the continental shelves of the east and west coasts of North America also indicate a sink of N^* due to benthic denitrification. High concentrations of N^* (>2.0 μmol kg^{-1}) indicative of prevailing nitrogen fixation are found in the thermocline of the tropical and subtropical North Atlantic and in the Mediterranean. This suggests that on a global scale these basins are acting as sources of fixed nitrogen, while the Indian Ocean and parts of the Pacific Ocean are acting as sinks. Nitrogen fixation is estimated in the North Atlantic Ocean (10°N–50°N) using the N^* distribution along isopycnal surfaces and information about the water age. We calculate a fixation rate of 28 Tg N yr^{-1} which is about 3 times larger than the most recent global estimate. Our result is in line, however, with some recent suggestions that pelagic nitrogen fixation may be seriously underestimated. The implied flux of 0.072 mol N m^{-2} yr^{-1} is sufficient to meet all the nitrogen requirement of the estimated net community production in the mixed layer during summer at the Bermuda Atlantic Time-series Study (BATS) site in the northwestern Sargasso Sea. Extrapolation of our North Atlantic estimate to the global ocean suggests that the present-day budget of nitrogen in the ocean may be in approximate balance.

Introduction

In the classical paradigm of biological oceanography, nitrogen is regarded as the limiting nutrient for phytoplankton growth and export production in most regions of today's ocean [*Codispoti*, 1989; *Smith*, 1984]. This contrasts with the view of geochemists, who regard phosphorus as the biolimiting nutrient on very long timescales. These different views are mainly caused by the different biogeochemical behavior of these two major nutrients. The amount of available fixed nitrogen (all forms of nitrogen except molecular nitrogen (N_2)) in the ocean can be changed by the biological processes of denitrification and nitrogen fixation, whereas the amount of phosphorus in the ocean (mainly in form of phosphate) is only affected by the balance between river input and loss to the sediments. The general consensus today is that while nitrogen fixation has probably kept up with the demand over timescales of the order of million of years, imbalances in the marine nitrogen budget in which denitrification exceeds nitrogen fixation over periods of several thousands years could change oceanic export production by significant amounts [*Codispoti*, 1989].

Several recent studies indicate that total oceanic denitrification is indeed exceeding total oceanic nitrogen fixation and hence that the ocean is loosing fixed nitrogen [*Codispoti*, 1995; *Ganeshram et al.*, 1995; *Codis-*

Paper number 97GB00077.
0886-6236/97/97GB-00077$12.00

poti and Christensen, 1985; *McElroy*, 1983]. *McElroy* [1983] pointed out that the present loss of fixed nitrogen may be linked with variations of the atmospheric CO_2 concentration between glacial and interglacial periods. He proposed that the oceans gain fixed nitrogen during glacial periods and lose it during interglacial periods. Higher amounts of nitrogen in the oceans during glacial periods would increase the strength of the biological carbon pumps [*Volk and Hoffert*, 1985] and thus lead to a decrease of atmospheric CO_2. The converse would occur during the interglacial periods. This mechanism would help to explain the observed changes in atmospheric CO_2 concentrations between the last glacial period and the present Holocene [*Neftel et al.*, 1982, 1988; *Staffelbach et al.*, 1991]. *Shaffer* [1990] elaborated this argument further by developing a simple biogeochemical model of ice age cycles which includes ocean denitrification explicitly.

However, large uncertainties exist in estimates of the marine nitrogen budget. While older studies suggested that the marine nitrogen cycle is approximately in steady state [*Liu*, 1979] or with an imbalance of order of 60 Tg N yr^{-1} (1 Tg = 10^{12} g) [*Codispoti and Christensen*, 1985] with total losses and sinks of the order of 100 Tg N yr^{-1}, more recent studies indicate a much more dynamic marine nitrogen cycle with total losses and sinks of the order of 200–300 Tg N yr^{-1} [*Galloway et al.*, 1995; *Codispoti*, 1995]. From the latter studies the mean oceanic residence time of nitrogen would decrease from about 10,000 years to approximately 3,000–5,000 years. All present estimates of the magnitude of the processes affecting the amount of nitrogen in the oceans are based on a small number of measurements, usually obtained over small temporal and spatial scales. Extrapolation of these data to the global scale has proven to be difficult [*Galloway et al.*, 1995], and therefore large ranges exist for the estimated rates of the different processes. Thus, at the moment it is not really possible to decide whether the oceanic nitrogen budget is in balance or not [*Codispoti*, 1995].

In this paper we use a new quasi-conservative tracer N^* to assess the marine nitrogen cycle. Our method is based on the large-scale distribution of nitrate and phosphate in the world ocean and therefore eliminates most of the problems associated with the extrapolation of sparse direct observations of nitrogen fixation and denitrification. N^* is defined as a linear combination of nitrate (N) and phosphate (P) of the form $N^* = N - r_{\mathrm{nitr}}^{N:P} P + \mathrm{const}$, where $r_{\mathrm{nitr}}^{N:P}$ is the constant N:P stoichiometric ratio during the remineralization of organic material (hitherto called nitrification) and where const is a constant to be determined. The idea is that this linear combination would eliminate most of the effect of nitrification of organic matter on nitrate and phosphate which is the most important contribution to the variability of these two tracers. The remaining variability of N^* is then primarily caused by the combined effect of denitrification and nitrogen fixation plus, to a smaller extent, atmospheric deposition and river inflow. We will show that this new quasi-conservative tracer depicts the known spatial distribution of denitrification and nitrogen fixation in a consistent manner. This leads us to conclude that our a priori assumption of a constant stoichiometric ratio during nitrification is reasonable for all investigated ocean regions. We will also demonstrate that a combination of N^* with ocean circulation tracers gives the opportunity to estimate average rates of denitrification and nitrogen fixation over large oceanic regions. This concept will be applied to the North Atlantic, where both high quality nutrient and circulation tracer observations are available.

Our concept of N^* is based on an idea of *Broecker and Peng* [1982, p. 139ff]. These authors calculated the nitrate deficit in the Indian Ocean and in the Bering Sea by multiplying the observed phosphate by the stoichiometric ratio of 15 and by subtracting this from the observed nitrate concentration. They did not attempt, however, to use the resulting tracer, which is basically equal to N^*, for a global investigation.

Fanning [1992] used an approach different to ours by investigating the global distribution of the N:P ratio and the occurrence of "ideal" covariation in the world oceans. Interpretation of the variations in the N:P ratio are difficult, however, because this ratio is highly nonlinear, especially at low nutrient concentrations, and therefore not conservative. Thus it is not possible to infer in a quantitative manner the large-scale distribution of marine denitrification and nitrogen fixation from analysis of the N:P ratios.

Naqvi and Sen Gupta [1985] proposed a different concept involving the conservative tracer "NO" [*Broecker*, 1974] to estimate nitrate deficits in the Arabian Sea caused by denitrification. This technique was later used successfully in a number of studies in that region [*Naqvi et al.*, 1990; *Mantoura et al.*, 1993]. However, NO is only conservative in the interior of the ocean and therefore can only be used to infer relative changes of NO after a water parcel has left contact with the atmosphere. It is therefore not possible to study the global scale distribution of denitrification and nitrogen fixation using this tracer.

The global extent of our study is limited by the availability of high-precision nutrient data from the Geochemical Ocean Sections Study (GEOSECS) program as well as from eight other programs in the Atlantic (Transient Tracers in the Ocean (TTO), South Atlantic Ventilation Experiment (SAVE), etc.). The observations presently being obtained by the World Ocean Circulation Experiment (WOCE) will soon provide the opportunity to investigate the distribution of N^* in more detail than was possible in this study.

The paper is organized as follows: In the first section we present the concept and mathematical derivation of N^*. We then describe briefly the data employed

in our study and provide an analysis of the error in our estimate of N^*. Then the results are presented as large-scale averages and as more detailed distributions in individual ocean basins. In the following section, we attempt to estimate the rate of nitrogen fixation in the tropical and subtropical North Atlantic based on the N^* distribution in this region. We then discuss our estimated nitrogen fixation rate in the Atlantic Ocean in light of the global marine nitrogen budget and possible implications for the marine carbon cycle and the atmospheric CO_2 concentration.

Concept of N^*

In the interior of the ocean, away from the surface euphotic layer, the biogeochemical cycles of nitrate (N) and phosphate (P) are mainly affected by mineralization of organic matter, but also by the processes of denitrification and mineralization of nitrogen-rich organic matter originating from organisms capable of N_2 fixation (diazotrophic organisms). For simplification, we refer to the whole remineralization process as nitrification, although organic nitrogen is first converted to ammonia (ammonification) and then in a second step is oxidized to nitrate (nitrification). The tracer continuity equation for nitrate and phosphate in the interior ocean can therefore be written as follows:

$$\Gamma(N) = J_{\text{nitr}}(N) + J_{\text{denitr}}(N) + J_{\text{N-rich nitr}}(N), \quad (1)$$

$$\Gamma(P) = J_{\text{nitr}}(P) + J_{\text{denitr}}(P) + J_{\text{N-rich nitr}}(P), \quad (2)$$

where J_{nitr} denotes the source minus sink term due to the remineralization of organic matter (nitrification), J_{denitr} denotes the source minus sink term due to denitrification, and $J_{\text{N-rich nitr}}$ denotes the source minus sink term due to the remineralization of nitrogen-rich organic matter from N_2 fixation. The operator Γ represents the transport and time rate of change:

$$\Gamma(T) = \frac{\partial T}{\partial t} + \vec{u} \cdot \nabla T - \nabla \cdot (D \cdot \nabla T), \quad (3)$$

where T denotes any tracer concentration, ∇ denotes the gradient operator in three dimensions, $\vec{u}$ denotes the velocity field, and D denotes the eddy diffusivity tensor.

Since we are specifically interested in the processes of denitrification and nitrification of nitrogen-rich organic matter from N_2 fixers, we would like to eliminate the effect of the mineralization of organic matter from the observations. We assume that during the process of nitrification, nitrate and phosphate are released with the stoichiometric ratio, $r_{\text{nitr}}^{N:P}$:

$$J_{\text{nitr}}(N) = r_{\text{nitr}}^{N:P}\, J_{\text{nitr}}(P). \quad (4)$$

In the case of denitrification and nitrification of nitrogen-rich organic matter the relationship between the cycling of phosphate and that of nitrate are given by the stoichiometric ratios $r_{\text{denitr}}^{N:P}$ and $r_{\text{N-rich nitr}}^{N:P}$, respectively:

$$J_{\text{denitr}}(N) = r_{\text{denitr}}^{N:P}\, J_{\text{denitr}}(P), \quad (5)$$

$$J_{\text{N-rich nitr}}(N) = r_{\text{N-rich nitr}}^{N:P}\, J_{\text{N-rich nitr}}(P). \quad (6)$$

Substituting these relationships ((4)-(6)) into (1) and (2) gives

$$\Gamma(N) = r_{\text{nitr}}^{N:P} J_{\text{nitr}}(P) + J_{\text{denitr}}(N) + J_{\text{N-rich nitr}}(N), \quad (7)$$

$$\Gamma(P) = J_{\text{nitr}}(P) + \frac{1}{r_{\text{denitr}}^{N:P}} J_{\text{denitr}}(N) + \frac{1}{r_{\text{N-rich nitr}}^{N:P}} J_{\text{N-rich nitr}}(N). \quad (8)$$

We can eliminate the nitrification term in (7) by subtracting $r_{\text{nitr}}^{N:P}\,\Gamma(P)$ from it :

$$\Gamma(N) - r_{\text{nitr}}^{N:P}\Gamma(P) = \left(1 - \frac{r_{\text{nitr}}^{N:P}}{r_{\text{denitr}}^{N:P}}\right) J_{\text{denitr}}(N) + \left(1 - \frac{r_{\text{nitr}}^{N:P}}{r_{\text{N-rich nitr}}^{N:P}}\right) J_{\text{N-rich nitr}}(N). \quad (9)$$

In the final step we take advantage of the fact that if one assumes a constant N:P ratio during nitrification ($r_{nitr}^{N:P}$), both the nitrate and phosphate equations are linear, and therefore the transport and time rate of change operators Γ can be combined to $\Gamma(N - r_{nitr}^{N:P}\, P)$. This permits us to define a new tracer N^*, whose interior distribution is only affected by transport, nitrification of nitrogen-rich organic matter, and denitrification:

$$N^* = (N - r_{\text{nitr}}^{N:P} P + \text{const}) \left(\frac{r_{\text{denitr}}^{N:P}}{r_{\text{denitr}}^{N:P} - r_{\text{nitr}}^{N:P}}\right), \quad (10)$$

$$\Gamma(N^*) = J_{\text{denitr}}(N) + \left(\frac{r_{\text{denitr}}^{N:P}}{r_{\text{denitr}}^{N:P} - r_{\text{nitr}}^{N:P}}\right) \left(\frac{r_{\text{N-rich nitr}}^{N:P} - r_{\text{nitr}}^{N:P}}{r_{\text{N-rich nitr}}^{N:P}}\right) J_{\text{N-rich nitr}}(N). \quad (11)$$

The final term in parentheses in (10) and (11) originates from the division of (9) by $(1 - r_{\text{nitr}}^{N:P}/r_{\text{denitr}}^{N:P})$ to obtain a tracer that directly reflects the source minus sink term of denitrification, $J_{\text{denitr}}(N)$.

In order to proceed we must first define the values of the stoichiometric ratios in (10). For $r_{\text{nitr}}^{N:P}$ we choose the Redfield ratio of 16:1 [*Redfield et al.*, 1963]. This value has been confirmed by *Takahashi et al.* [1985] and *Anderson and Sarmiento* [1994] who obtained a value of 16 ± 1. These authors also showed that N:P is noticeably smaller in the 1000-3000 m depth zone (around 12), but similar in the 3000-4000 m zone (around 15). Similar findings were obtained by *Peng and Broecker* [1987], *Minster and Boulahdid* [1987], and *Boulahdid and Minster* [1989]. *Anderson and Sarmiento* [1994] concluded that the N:P ratio for the mineralization of organic matter is in fact around 16, and they attributed these lower ratios to the effect of denitrification. *Min-*

ster and Boulahdid [1987] suggested that perhaps N is actually more rapidly recycled than P, but there is little evidence for this and much in support for the contrary. We will address this topic further in the discussion section.

The N:P ratio during denitrification was evaluated from the reaction equation of denitrification coupled with the mineralization of organic matter with a typical elementary composition of surface ocean phytoplankton [*Anderson*, 1995] :

$$C_{106}H_{175}O_{42}N_{16}P + 104\,NO_3^- = 4\,CO_2 + 102\,HCO_3^- + 60\,N_2 + 36\,H_2O + HPO_4^{2-} \quad (12)$$

According to this equation a value of −104 for $r^{N:P}_{\text{denitr}}$ was chosen for our calculations. The carbon stoichiometry of the remineralization reaction of organic matter below 400 m is somewhat higher than that of surface ocean phytoplankton: C:N:P = 117±14:16±1:1 [*Anderson and Sarmiento*, 1994]. However, since we lack the organic H and O components in deep ocean organic matter, it is not possible to work out the stoichiometry of the denitrification reaction there exactly. If we assume that the hydrogen content of the deep organic matter is increased by 33 relative to the composition in surface ocean water, which is in proportion to the increase in carbon, and that the organic oxygen content remains the same, the N:P ratio for denitrification $r^{N:P}_{\text{denitr}}$ would change by 11 to −115. Our estimates are very similar to *Naqvi et al.* [1990], who estimated $r^{N:P}_{\text{denitr}}$ to be −108.8 based on the stoichiometry of *Takahashi et al.* [1985] and assuming a nitrification-denitrification couple to be operational [*Codispoti and Christensen*, 1985]. However, the C:H:O content of the organic matter in the study of *Naqvi et al.* [1990] was very different, and therefore this agreement is rather accidental. *Smethie* [1987] calculated for $r^{N:P}_{\text{denitr}}$ a value of 94.4 also under the assumption of a close coupling between nitrification and denitrification. On the basis of the work of *Anderson* [1995] we tentatively estimate the error $\sigma_{r^{N:P}_{\text{denitr}}}$ of $r^{N:P}_{\text{denitr}}$ to be about ±15 which encompasses all other estimates.

Very few measurements exist for the N:P ratio in nitrogen-rich organic matter produced by diazotrophic organisms ($r^{N:P}_{\text{N-rich nitr}}$). We will employ a value of 125 based on observations during a *Trichodesmium* bloom in the Pacific near Hawaii [*Karl et al.*, 1992]. This estimate is very uncertain. Fortunately, the value of $r^{N:P}_{\text{N-rich nitr}}$ has no influence on the value or distribution of N^*. It is only important if we want to calculate the source minus sink term $J_{\text{N-rich nitr}}$ (see below).

Using these values for the N:P ratios, the definition of N^* finally simplifies to

$$N^* = (N - 16P + 2.90\ \mu\text{mol kg}^{-1})\ 0.87, \quad (13)$$

$$\Gamma(N^*) = J_{\text{denitr}}(N) + 0.76\ J_{\text{N-rich nitr}}(N). \quad (14)$$

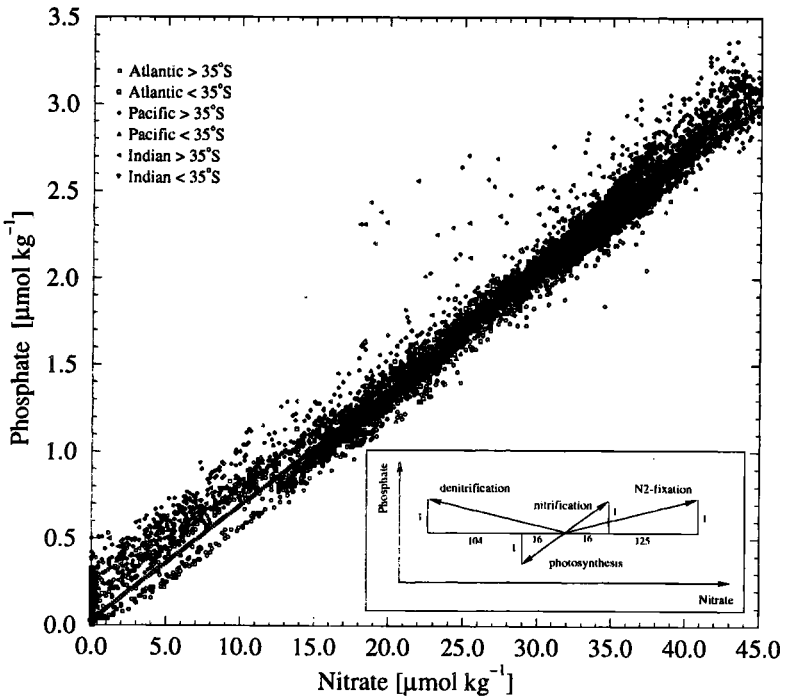

Figure 1. Plot of phosphate versus nitrate based on data from the GEOSECS cruises and all depths. The inset shows the effect of nitrification, photosynthesis, N_2 fixation, and denitrification in this P versus N diagram (not to scale). The solid line shows the linear equation $P = 1/16\ N + 0.182$, which is the result of setting N^* in (13) to zero and solving for P. Values on the right side of this line are equivalent to positive N^*, whereas values on the left side reflect negative N^*.

We determined the constant (2.90 μmol kg^{-1}) in (13) by forcing the global mean of N^* based on GEOSECS data (see below) to be zero. This value for the constant equals the value that would be calculated using the GEOSECS-based global mean nitrate of 30.38 μmol kg^{-1} and global mean phosphate of 2.08 μmol kg^{-1}. On the global scale an excess of phosphate compared to the ideal covariation with nitrate exists, and one can therefore speculate that favorable conditions for N_2 fixation are provided.

N^* can also be understood as the deviation from the solid line in Figure 1, where phosphate is plotted against nitrate based on all GEOSECS observations. This line has been determined by setting N^* in (13) to zero and then solving for P which results in the linear equation $P = 1/16N + 0.182$. The constant in the latter equation reflects again the difference between global mean nitrate and 16 times global mean phosphate. Values on the right side of the line in Figure 1 are equivalent to positive N^*, whereas values on the left side of this line reflect negative N^*. The insert in this figure shows how the three processes nitrification, denitrification, and nitrification of high N:P organic matter influence the nutrient concentrations in this P versus N plot.

Since denitrification and N_2 fixation occur only in very limited regions of the world oceans, $J_{\text{denitr}}(N)$ and $J_{\text{N-rich nitr}}$ are mostly zero, and therefore N^* should have, for the major part of the ocean, conservative properties with a global mean of zero. In the other regions, N^* reflects the balance between denitrification and 0.76 times the nitrification of nitrogen-rich organic matter generated by N_2 fixers. It is important to note here that the absolute value of N^* is arbitrary. Therefore negative values cannot be directly associated with denitrification nor positive values with N_2 fixation. Only a change in N^* which deviates from a conservative behavior can be interpreted as the net effect of denitrification and N_2 fixation.

Data Considerations

To investigate the distribution of N^* on a global scale, we use nutrient data from the Geochemical Ocean Sections Study (GEOSECS) program (1972-1978) [*Bainbridge*, 1981; *Broecker et al.*, 1982; *Weiss et al.*, 1983]. The station locations are shown in Figure 2. Various corrections were applied to the GEOSECS phosphate data as discussed by *Broecker et al.* [1985, Table 2] and summarized by *Anderson and Sarmiento* [1994].

In the Atlantic Ocean we also use nutrient data from the Transient Tracers in the Oceans North and Tropical Atlantic Studies ((TTO NAS) and (TTO TAS), respectively) [*Physical and Chemical Oceanographic Data Facility (PCODF)*, 1986a, b], the South Atlantic Ventilation Experiment (SAVE) [*Oceanographic Data Facility (ODF)*, 1992a, b], Atlantis II cruise 109 [*Roemmich and Wunsch*, 1985], Oceanus cruise 133, leg 7 [*World Ocean*

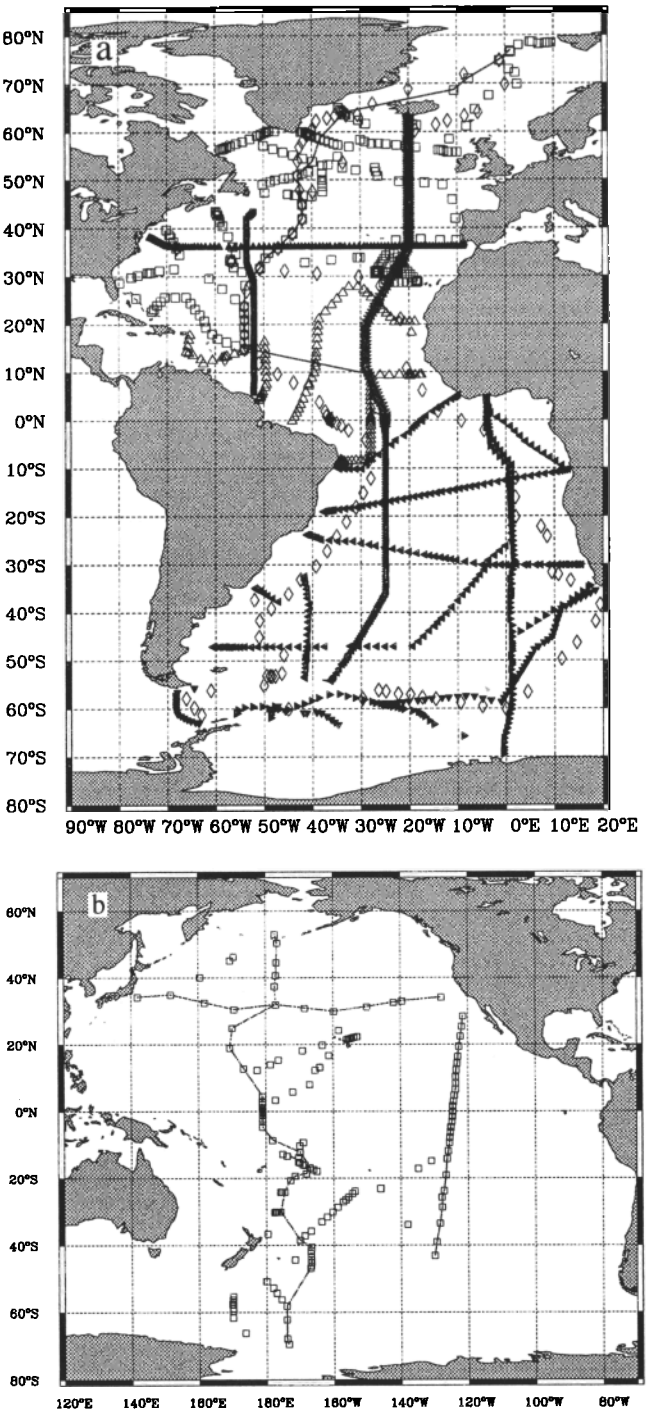

Figure 2. Hydrographic station locations as used in our study. (a) Station locations in the Atlantic Ocean. Open squares, stations from TTO NAS (1981); triangles, stations from TTO TAS (1983); diamonds, stations from GEOSECS (1972-1973); stars, stations from Oceanus 202 (1988); solid squares, stations from Oceanus 133-7 (1983); upward pointing triangles, stations from Atlantis 109 (1981); leftward pointing triangles, stations from SAVE(1987-1989); downward pointing triangles, stations from *Meteor* 11/5 (1991); rightward pointing triangles, stations from AJAX (1983-84) (b) Station locations of the GEOSECS Pacific cruises (1973/1974) (c) Station locations of the GEOSECS Indian cruises (1977/1978).

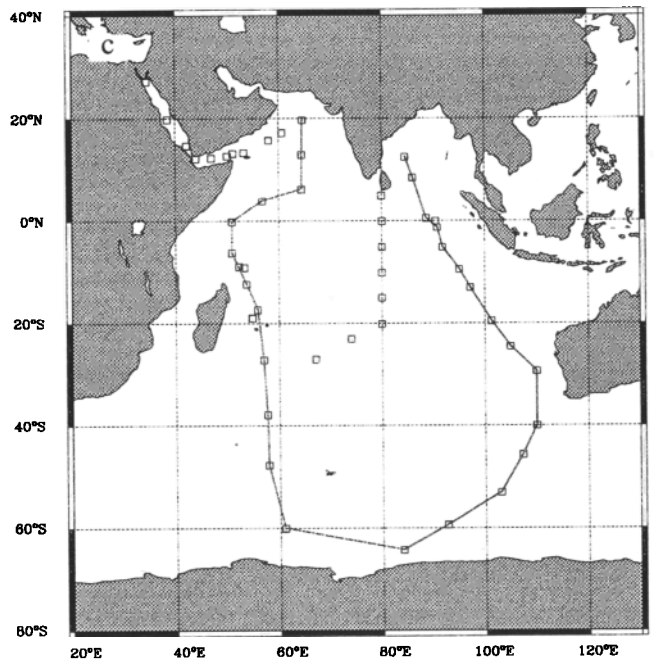

Figure 2. (continued)

Circulation Experiment Hydrographic Programme Special Analysis Centre (WHP SAC), 1996a], Oceanus cruise 202 (World Ocean Circulation Experiment (WOCE) leg A16N) [*World Ocean Circulation Experiment Hydrographic Programme Special Analysis Centre (WHP SAC)*, 1996b], the AJAX Long Lines cruises, and the *Meteor* 11/5 cruise (WOCE legs A12/A21) [*Chipman et al.*, 1994]. These cruises provide good spatial coverage of the North and South Atlantic Ocean with high-quality nutrient data (see Figure 2 for station locations). Internal consistency of the different data sets is crucial in the analysis of N^*, since we are looking for small deviations in the N and P fields. We checked the internal consistency of the nutrient data by investigating deep ocean (>3500 m) N and P trends versus potential temperature at (1) reoccupied or closely revisited stations and in (2) 10° latitude by 10° longitude regions that have been repeatedly sampled by the different cruises. We found internally consistent nutrient data between the GEOSECS, TTO NAS, TTO TAS, SAVE, Atlantis 109, and AJAX cruises. Oceanus 202, Oceanus 133-7, and *Meteor* 11/5 , however, showed systematic differences which were corrected (see the appendix for details).

The GEOSECS (1972-1973), TTO (1981-1983), Oceanus 133-7 (1983), Atlantis 109 (1981), SAVE (1987-1989), Oceanus 202 (1988), AJAX (1983-1984) and *Meteor* 11/5 (1991) cruises span a period of about 20 years (10 years without GEOSECS). Comparison of reoccupied stations between the different cruises revealed mostly no significant systematic differences in water mass characteristics. However, temporal variability was noted by *Broecker* [1985] and *Swift* [1984] for the decade between 1972 and 1982 for the water masses south of Greenland. *Brewer et al.* [1983] detected a significant and widespread freshening of the deep waters in the subpolar North Atlantic between 1962 and 1981. *Coles et al.* [1996] reported changes in the water mass characteristics of the Antarctic Bottom Water in the Argentine basin between 1980 and 1989. We also observed changes in the potential temperature versus salinity diagrams for waters in the lower limb of the Antarctic Intermediate Water in the Brazil Basin between approximately 15°S and 25°S between 1972 and 1989. However, these observed temporal changes in water masses are an order of magnitude smaller than the spatial variability that is our primary focus. We therefore neglect this temporal variability and combine the data sets as if they were synoptic.

Arsenate positively interferes with colorimetric determination of phosphate [*Johnson and Pilson*, 1972]. *Fanning* [1992] decided to reduce all GEOSECS and TTO phosphate data by a constant of 0.02 μmol kg^{-1}, based on arsenate observations in oligotrophic surface and middepth waters. We apply no such correction to our phosphate data, first, because the distribution of arsenate is not well known in the world oceans and therefore any chosen constant value is somewhat tentative; and second and more important, because a constant reduction of the phosphate concentration changes only the value of the constant in the definition of N^* (see equation (13)) and not the structure or range of N^* itself.

The evaluation of the distribution of N^* also requires estimates of the variations that arise as a consequence of errors in the estimate of the $N{:}P$ nitrification and denitrification ratios ($\sigma_{r^{N:P}_{\text{nitr}}}$ and $\sigma_{r^{N:P}_{\text{denitr}}}$, respectively) and errors during nutrient sampling and measurement (σ_N and σ_P, respectively). Assuming that the analytical determinations for phosphate and nitrate and the estimates of the $N{:}P$ ratios are unrelated, the associated errors are independent and uncorrelated. The error of N^*, σ_{N^*} can therefore be calculated by error propagation:

$$\sigma^2_{N^*} = \left(\frac{\partial N^*}{\partial N}\sigma_N\right)^2 + \left(\frac{\partial N^*}{\partial P}\sigma_P\right)^2 + \left(\frac{\partial N^*}{\partial r^{N:P}_{\text{nitr}}}\sigma_{r^{N:P}_{\text{nitr}}}\right)^2 + \left(\frac{\partial N^*}{\partial r^{N:P}_{\text{denitr}}}\sigma_{r^{N:P}_{\text{denitr}}}\right)^2, \quad (15)$$

$$= \left(\frac{r^{N:P}_{\text{denitr}}}{r^{N:P}_{\text{denitr}} - r^{N:P}_{\text{nitr}}}\,\sigma_N\right)^2 + \left(\frac{r^{N:P}_{\text{denitr}}}{r^{N:P}_{\text{denitr}} - r^{N:P}_{\text{nitr}}}\,r^{N:P}_{\text{nitr}}\,\sigma_P\right)^2 + \left(\frac{r^{N:P}_{\text{denitr}}}{r^{N\,P}_{\text{denitr}} - r^{N\,P}_{\text{nitr}}}\right.$$

$$\left(-P + \frac{N - r^{N:P}_{\text{nitr}} P + \text{const}}{r^{N:P}_{\text{denitr}} - r^{N:P}_{\text{nitr}}}\right) \sigma_{r^{N:P}_{\text{nitr}}}\Bigg)^2 + \Bigg(\left(N - r^{N:P}_{\text{nitr}} P + \text{const}\right) \frac{-r^{N:P}_{\text{nitr}}}{\left(r^{N:P}_{\text{denitr}} - r^{N:P}_{\text{nitr}}\right)^2} \sigma_{r^{N:P}_{\text{denitr}}}\Bigg)^2 . \quad (16)$$

Inserting the values of the N:P ratios in the above equation for σ_{N^*} yields

$$\sigma^2_{N^*} = (0.8667\,\sigma_N)^2 + (13.867\,\sigma_P)^2 + \left(0.8667\left(-P - \frac{N - 16P + 2.90}{120}\right)\sigma_{r^{N:P}_{\text{nitr}}}\right)^2 + \left((N - 16P + 2.90)\,(-0.00111)\,\sigma_{r^{N:P}_{\text{denitr}}}\right)^2 . \quad (17)$$

The error of N^* is dependent on the phosphate and nitrate concentrations. In Figure 3 the error of N^* is shown as a function of depth based on the global horizontal mean phosphate and nitrate concentration profile, and conservative error estimates of $\sigma_N = 0.2$ μmol kg^{-1}, $\sigma_P = 0.02$ μmol kg^{-1}, $\sigma_{r^{N:P}_{\text{nitr}}} = 1$, and $\sigma_{r^{N:P}_{\text{denitr}}} = 15$. Nutrient concentrations at the surface are low, and the error of N^* is about 0.5 μmol kg^{-1}, influenced equally by the error of the nutrient analysis and the error in the N:P ratio of nitrification. Progressing downward, nutrient concentrations increase, and in the waters below 1000 m the calculated error of N^* is between 1.9 and 2.0 μmol kg^{-1}, controlled almost entirely by the error in the N:P ratio of nitrification, $\sigma_{r^{N:P}_{\text{nitr}}}$. However, interleg and intercruise comparison of reoccupied and closely revisited stations in the Atlantic Ocean shows that the deep water error of N^* is probably significantly smaller, implying a smaller error of the deep water N:P denitrification ratio. The mean squared difference of N^* for 35 station pairs in the Atlantic is calculated as 0.65 μmol kg^{-1}, supporting a value of only 0.25 for $\sigma_{r^{N:P}_{\text{nitr}}}$ in the deep ocean. Using this uncertainty estimate in the surface waters as well, the error of N^* decreases only slightly to about 0.3 μmol kg^{-1} (Figure 3). On the basis of this analysis and the estimate from the error propagation we estimate the error of N^*, σ_{N^*}, to be of order 0.7 μmol kg^{-1}. Our analysis above does not include potential biases because of systematic or correlated errors. Such errors are very difficult to assess, and we tried to minimize them by carefully investigating the internal consistency of all nutrient data and applying corrections where necessary.

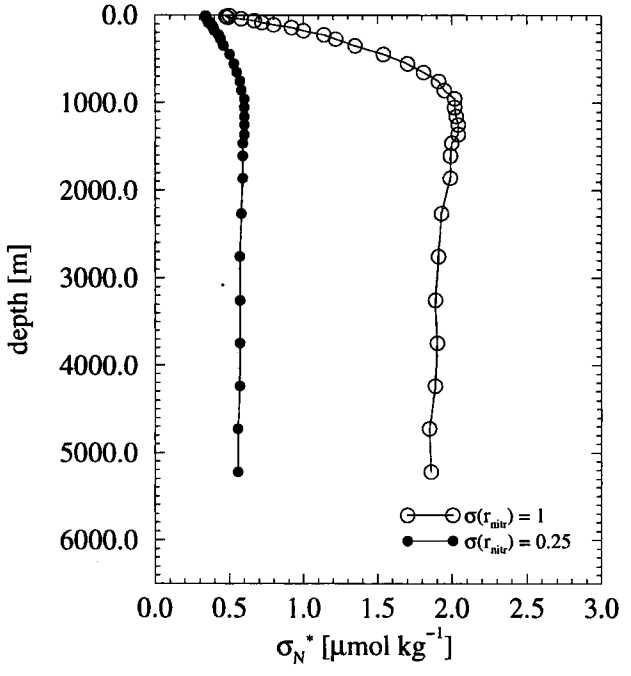

Figure 3. Plot of the error of N^*, σ_{N^*} versus depth for two different estimates of the uncertainty in the N:P nitrification ratio, $r^{N:P}_{\text{nitr}}$ (see equation (17)).

To prepare tracer plots on isopycnal surfaces, all quantities were linearly interpolated from levels of observations to potential density surfaces. Potential density was calculated using the United Nations Educational, Scientific, and Cultural Organization (UNESCO) equation of state for seawater [UNESCO, 1981] together with *Fofonoff's* [1977] algorithm for calculating potential temperature and the formula of *Bryden* [1973] for the adiabatic temperature gradient. The line of wintertime outcrop for each surface was determined from the National Oceanic and Atmospheric Administration (NOAA) National Environmental Satellite Data and Information Service (NESDIS) ocean atlas [*Levitus et al.*, 1994; *Levitus and Boyer*, 1994b] for each hemisphere, and those stations lying poleward of outcrops were excluded. Randomly distributed data were gridded onto a 1° grid using the objective mapping technique described by *LeTraon* [1990]. We used an autocorrelation function of gaussian form, with a 1200 km radius of influence in the meridional as well as zonal direction. This objective mapping technique is very similar to that developed and described by *Sarmiento et al.* [1982]. The LeTraon technique gives a somewhat larger error because it simultaneously estimates the large-scale and the mesoscale components with an accurate error budget, whereas Sarmiento et al.'s technique takes into account only the error of the mesoscale component.

Global Observations

Horizontal Mean Profiles of N^*

We calculated the horizontal mean N^* obtained from GEOSECS observations in the Atlantic, Pacific, and Indian Oceans north and and south of 35°S (see Figure 4). This boundary has been chosen because this is the latitude of the southern tips of Africa and Australia and is

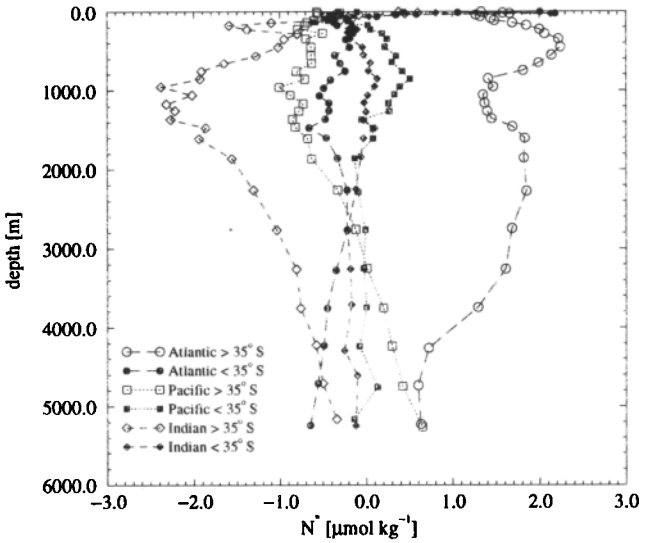

Figure 4. Horizontally average profiles of N^* in the world oceans based on GEOSECS data. Each ocean basin has been split into a part north of 35°S (open symbols) and a part representing the Southern Ocean south of 35°S (solid symbols).

therefore the northernmost possible boundary for separating the Southern Ocean from the rest of the basins. The deepest waters below 4500 m are roughly constant at a value of zero within the error margins. However, above this depth the basins show large differences. The Atlantic north of 35°S has consistently high values of around 1–2 μmol kg^{-1}. The maximum is at approximately 500 m. A local minimum exists between 1000 and 1500 m, possibly associated with Antarctic Intermediate Water. The higher values in the depth range between 1500 and 3000 m are in the North Atlantic Deep Water. The Pacific shows rather uniform values of around −0.8 μmol kg^{-1} in the upper 2000 m then increases steadily to about 0.7 μmol kg^{-1} below 5000 m. The Indian Ocean north of 35°S has very low values of between −1 and −3 μmol kg^{-1}, with the minimum occurring between 1000 and 1500 m. The upper 200 m, however, are characterized by positive N^* values reaching 0.5 μmol kg^{-1}. The vertical profiles of N^* in the Southern Ocean are approximately constant at around 0 μmol kg^{-1}, except for the upper 100 m in the Atlantic and Indian sector, where N^* increases above 1 μmol kg^{-1}.

These results suggest that the Atlantic is a major source of nitrate via N_2 fixation, and that the Indian Ocean acts a major sink relative to the other basins, at least below 200 m. Is this consistent with our expectations based on direct studies of these processes?

Since denitrification is inhibited by oxygen [*Hattori*, 1983], only water masses or microzones lacking oxygen can be potential sites of denitrification. The major areas of anoxia within the water column of the oceans are the thermocline of the Arabian Sea and the eastern tropical North and South Pacific [*Broecker and Peng*, 1982; *Anderson et al.*, 1982, p. 145] (see Figure 5). Many studies have confirmed that intense denitrification is occurring in these regions (see, e.g., *Hattori* [1983] for a review). Anoxic sediments have also been shown to be important sites of denitrification [e.g., *Christensen et al.*, 1987a, b]). N_2 fixation has been observed in all ocean basins, with maximum rates in the Indian Ocean, intermediate rates in the Atlantic, and minor rates in the Pacific [*Capone and Carpenter*, 1982]. For a more detailed analysis of the distribution of N^* we turn to a set of sections of N^* within these basins.

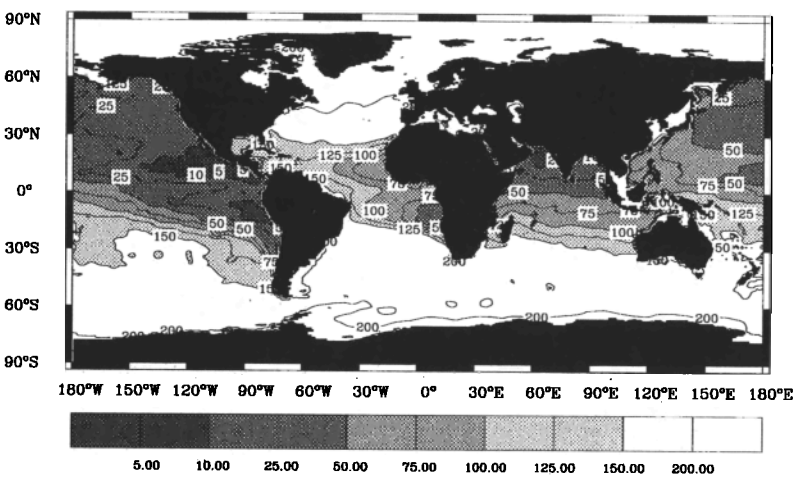

Figure 5. Global distribution of the dissolved oxygen concentration (micromoles per kilogram) at the depth of the vertical oxygen minimum. This plot has been constructed from the 1° gridded oxygen data of *Levitus and Boyer* [1994a].

Indian Ocean

The western Indian GEOSECS section, shown in Figure 6, shows a substantial N^* minimum in the Arabian Sea (see Figure 2c for track). The region of N^* values below -2.5 μmol kg^{-1} is confined to north of 10°S and to depth levels between 100 and 2700 m. It is associated with the oxygen depleted zone (ODZ) within the North Indian high-salinity intermediate waters [*Wyrtki*, 1988]. This ODZ, which contains essentially no detectable oxygen, is confined to the northeast Arabian Sea (east of 56°E) up to the Indian Continental shelf. It extends southward from the Gulf of Oman to about 12°N [*Naqvi*, 1987] and was thus transected by the GEOSECS section. The N^* minimum at the northernmost station is about -13 μmol kg^{-1} at a depth of 320 m, the lowest value found in our data set of the world oceans. Between 10°N and 20°N the core of these low N^* values is situated in the upper thermocline between 200 and 800 m, sharply separated from the surface waters. Between the equator and 10°N, N^* shows a rather sharp front in the depth range between 100 and 500 m that coincides with the occurrence of oxygen concentrations above 10 μmol kg^{-1} (not shown). Below this front the core of the low N^* values (< -2.5 μmol kg^{-1}) stretches southward at depths between approximately 500 and 1500 m until about 10°S, associated with the North Indian high-salinity Intermediate Water.

A large number of studies have investigated denitrification in the oxygen-depleted zone of the Intermediate Waters of the Arabian Sea (see reviews by *Naqvi* [1987] and *Burkill et al.* [1993]). The lowest N^* values are clearly found within this ODZ, but advection and diffusion transport the low N^* values to outside the ODZ. This large nitrate deficit as expressed in our analysis by very low N^* values has already been noted by *Sen Gupta et al.* [1976] and *Deuser et al.* [1978]. *Naqvi and Sen Gupta* [1985], *Naqvi et al.* [1990], and *Mantoura et al.* [1993] used a similar quasi-conservative tracer, NO [*Broecker*, 1974], to calculate the nitrate deficits in this region. *Mantoura et al.* [1993] found a distribution of nitrate deficit (which is approximately equivalent to N^*) very similar to ours on a section between the equator and 20°N following the 67°E longitude.

By contrast, the Indian Central Water, which is dynamically separated from the waters of the Arabian Sea by a front between 10°S and 20°S [*Wyrtki*, 1988], exhibits N^* concentrations around 0 to -0.5 μmol kg^{-1} (Figure 6). The Antarctic Intermediate Waters and the Indian Deep and Bottom Waters also have values in the same range. In the surface waters around 20°S, higher concentrations of N^* can be found, possibly associated with nitrogen fixation. The strong gradient between the low N^* waters in the ODZ in the Arabian Sea and the overlying surface waters may also be the result of nitrogen fixation because one would otherwise expect

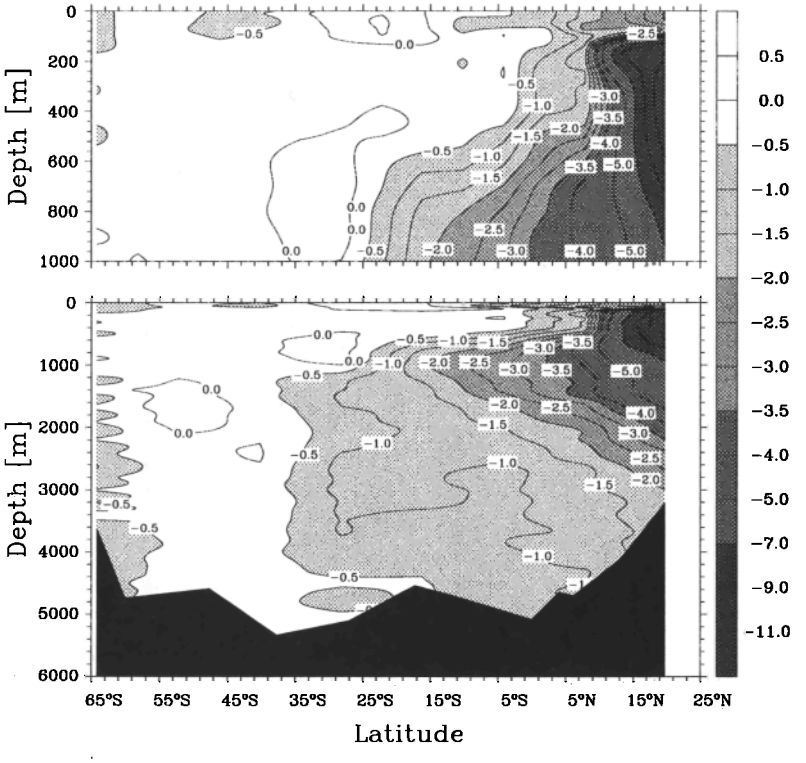

Figure 6. Meridional section of N^* (micromoles per kilogram) in the western Indian Ocean based on the GEOSECS Indian Expedition (1977/1978). See Figure 2 for the station locations.

that diffusion and advection of the very low N^* values would wipe out this gradient. This would be consistent with the known high rates of N_2 fixation in the Indian Ocean. *Carpenter* [1983] estimated that about two thirds of the global water column nitrogen fixation is occurring in this basin based on a compilation of the abundances of the marine diazotrophic cyanobacterium *Trichodesmium spp.* (presumably the main diazotroph in marine plankton). *Capone et al.* [1996] observed an extensive bloom of *Trichodesmium* with highly elevated nitrogen fixation rates. These high rates of N_2 fixation should lead to significant nonconservative changes in N^* in the water column. We consistently observe higher N^* concentrations near the surface at certain locations, but they are much smaller than the N^* values observed in the Atlantic Ocean. This does not necessarily indicate that N_2 fixation is smaller in the Indian Ocean than in the Atlantic. However our analysis suggests that the effect of denitrification in the northern basins of the Indian Ocean is overwhelming the effect of N_2 fixation, making the Indian Ocean a net sink rather than a net source of fixed nitrogen.

A very similar distribution of N^* can be found in the eastern Indian GEOSECS section (Figure 7). N^* values below -2.5 μmol kg^{-1} can again be found north of 15°S in the depth range between 200 and 2000 m associated with the North Indian high-salinity Intermediate water. The surface waters of the South Indian subtropical gyre between 30°S and 20°S and of the northernmost station in the Bay of Bengal show higher N^* values, supporting our previous findings about the role of nitrogen fixation in the Indian Ocean. The other water masses in the Indian Ocean as sampled by the eastern line show N^* values between 0 and -0.5 μmol kg^{-1} consistent with the observations along the western line.

Denitrification in the Bay of Bengal has not been studied as extensively as in the Arabian Sea [*Naqvi et al.*, 1978]. *Hattori* [1983] speculated that the Bay of Bengal may contribute to oceanic denitrification, as oxygen concentrations of less than 20 μmol kg^{-1} have been observed [*Wyrtki*, 1988]. Without a more detailed mapping of N^* in the Bay of Bengal it is not possible to decide whether the low N^* values we found are a remnant signal of denitrification in the Arabian Sea which has been mixed in with the North Indian high-salinity Intermediate Water, or if these low values are due to in situ denitrification.

To summarize, we find a strong N^* minimum in the ODZ of the Arabian Sea where denitrification is well studied. N^* shows elevated concentrations in the near surface waters possibly due to shallow nitrification of nitrogen-rich organic matter from diazotrophs, which are known to be abundant. Outside these regions, N^* behaves conservatively. All these findings are consistent with the available in situ observations and therefore support the concept of N^*. Our observations are

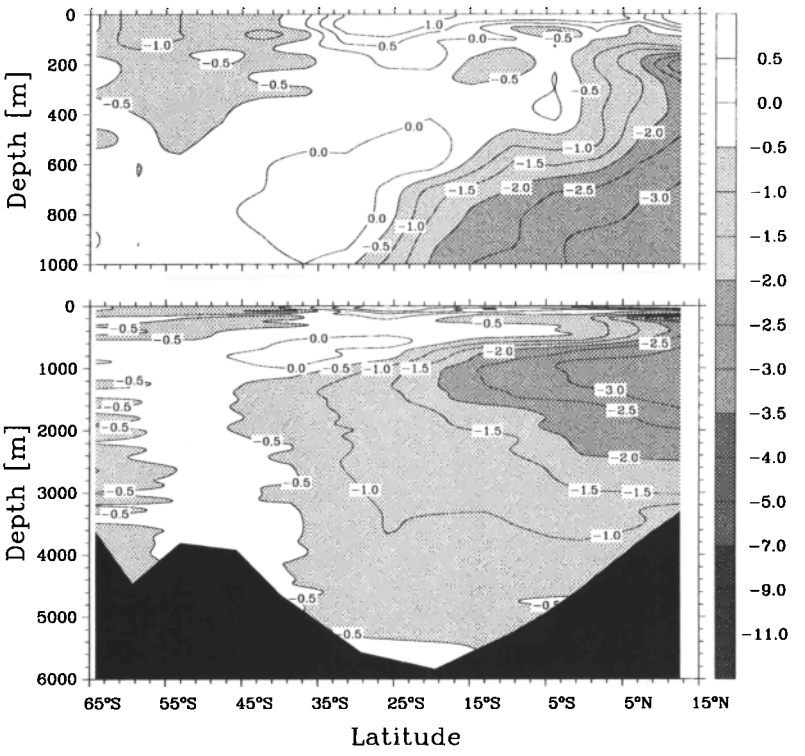

Figure 7. Meridional section of N^* (micromoles per kilogram) in the eastern Indian Ocean based on the GEOSECS Indian Expedition (1977/1978) See Figure 2 for the station locations.

also consistent with the conclusion of *Anderson and Sarmiento* [1994], who attributed the low N:P remineralization ratios found at middepth to denitrification.

Pacific Ocean

Unlike in the Indian Ocean, N^* shows much less variability in the Pacific GEOSECS sections (Figures 8-10). Although these sections are more noisy than the Indian Ocean sections, some clear trends can be discerned:

Distinct N^* minima can be found in the surface and deep waters of the Bering Sea (–3 to –4 μmol kg^{-1}) (Figure 8), in the thermocline of the eastern Pacific between 100 and 400 m and at about 15°N–20°N (–12 μmol kg^{-1}) (Figure 9) and in the middepth waters of the eastern North Pacific close to the American continent and between 600 and 2000 m (Figure 10). Note that the southward spreading of the Bering Sea signature in Figure 8 between 2000 and 4000 m is an artifact of the rather strong smoothing applied in the contouring program. A fourth N^* minimum can be found south of the equator between 5°S and 15°S (Figures 8 and 9). There is little variation of N^* outside these minima: the deep and bottom waters of the Pacific have N^* concentrations around –0.5 to 0 μmol kg^{-1} in the south, slightly increasing toward the north where typical values of 0.5 μmol kg^{-1} are found.

Does the N^* distribution reflect our expectations based on the knowledge of the nitrogen cycle in the Pacific Ocean? The N^* minima described above are clearly associated with oxygen minima with the exception of the Bering Sea and the middepth waters in the eastern North Pacific. The oxygen minimum zones in the Pacific Ocean are located in the eastern tropical North and South Pacific (ETNP and ETSP, respectively). Denitrification in these two regions has been well studied since *Brandhorst* [1959] first noted the presence of a secondary nitrite minimum due to denitrification (see *Thomas* [1966], *Goering et al.* [1973], *Cline and Richards* [1972], *Codispoti and Richards* [1976], and *Hattori* [1983] for the ETNP and *Fiadeiro and Strickland* [1968], *Codispoti and Packard* [1980], *Anderson et al.* [1982], and *Codispoti et al.* [1986] for the ETSP) Unfortunately, the GEOSECS Pacific cruises did not go east of 120°W, and therefore only an incomplete picture of the distribution of N^* in these oxygen minimum zones can be gained from the GEOSECS data alone

We use the objectively analyzed annual mean nitrate and phosphate fields of the NOAA NESDIS atlas [*Conkright et al.*, 1994] to study the distribution of N^* within the ETNP and ETSP regions. We did not use these data any further because *Conkright et al* [1994] combined data of very different quality and analysis precision for preparing the objectively analyzed nutrient fields. Furthermore, the calculation of N^* based on objectively mapped nutrient data leads to peculiar minima and maxima in regions with poor data cover-

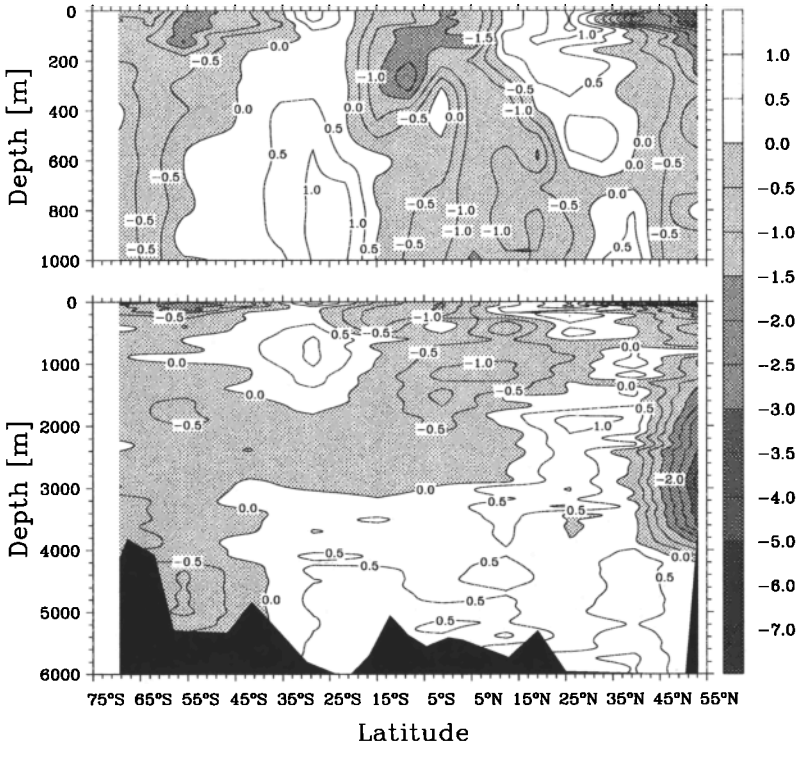

Figure 8. Meridional section of N^* (micromoles per kilogram) in the western Pacific Ocean based on the GEOSECS Pacific Expedition (1973/1974). See Figure 2 for the station locations.

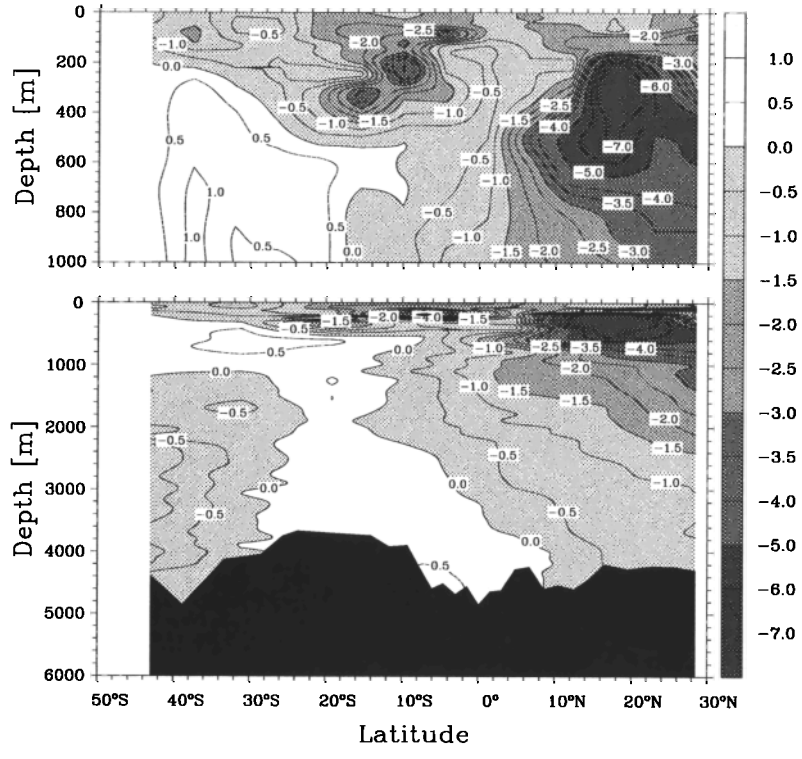

Figure 9. Meridional section of N^* (micromoles per kilogram) in the eastern Pacific Ocean based on the GEOSECS Pacific Expedition (1973/1974). See Figure 2 for the station locations.

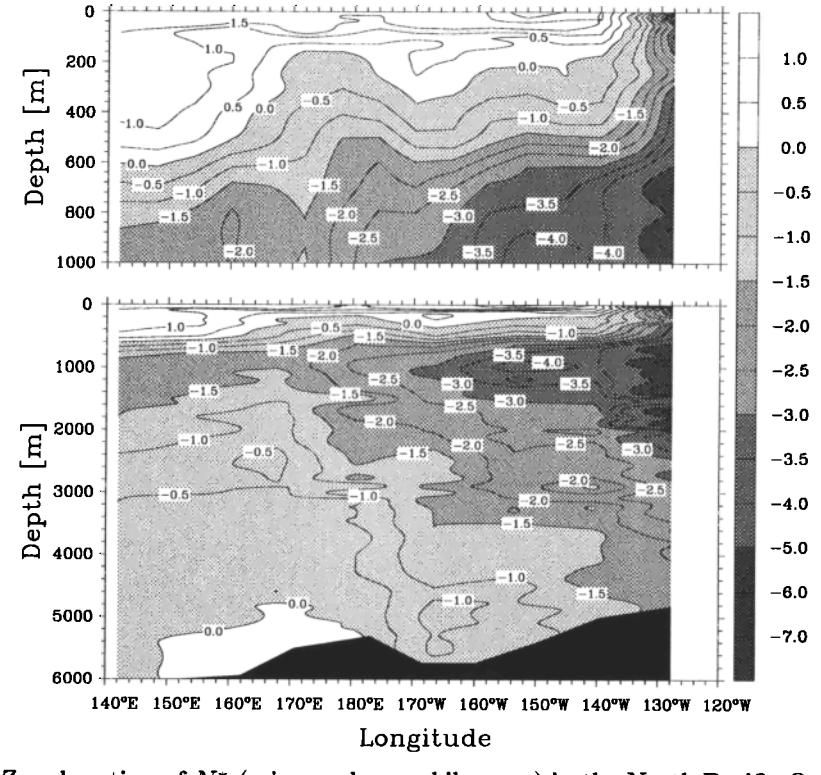

Figure 10. Zonal section of N^* (micromoles per kilogram) in the North Pacific Ocean based on the GEOSECS Pacific Expedition (1973/1974). See Figure 2 for the station locations.

age. Figure 11, where N^* is plotted at a depth of 200 m based on the NOAA NESDIS atlas, reveals two large tongues of low N^* extending westward from the oxygen minimum zones in the eastern tropical North and South Pacific. The core of the northern tongue is situated at a depth of about 200–300 m, in good agreement with the GEOSECS data. The core of the tongue is at about 15°N and extends westward from Central America to 180°W. The minima in the tongue are below −12 μmol kg^{-1}. Close to the west coast of Central America, the zone of low N^* values extends below 1000 m, whereas in the central Pacific, low N^* values can only be found in the upper 1000 m (not shown). The southern tongue is much smaller. The core of the tongue is between 30°S and 5°S, and it extends from the South American coast to about 120°W. The eastern GEOSECS section cuts through the core of the northern low N^* tongue but only touches the southern core, confirming our preliminary analysis above. The influence of the northern tongue can be seen only partially in the western section by a small local minimum between 5°S and 15°N. Thus the spatial distribution of these distinct N^* minima in the water column of the Pacific Ocean are clearly the result of denitrification in these oxygen minimum zones.

By contrast, the low N^* values found in the Bering Sea are not due to denitrification in the water column but probably due to denitrification in the sediments. *Koike and Hattori* [1979], *Tsunogai et al.* [1979], and *Haines et al.* [1981] estimated large denitrification rates in the sediments of the shelf and of the deeper basin. Although only one station was sampled within the Bering Sea (station 219) by the GEOSECS cruise, the very low N^* values found at that station are consistent with the findings of these studies.

Benthic denitrification which has been documented for the Santa Barbara Basin [*Barnes et al.*, 1975] and for the region off the coast of Washington near the delta of the Columbia river [*Christensen et al.*, 1987b; *Devol*, 1991] shows up as consistently lower N^* concentrations close to the continental margins in the northeastern Pacific in the N^* distribution in the upper 1000 m based on the NOAA NESDIS data [*Conkright et al.*, 1994] (see Figure 11). It also helps to explain the low mid-depth N^* values found at 30°N in the eastern part of that basin (Figure 10).

The near conservative distribution of N^* in the Pacific Ocean outside the sites of known denitrification indicates that either N_2 fixation is small or that denitrification in anoxic microenvironments is large enough to be approximately in balance with N_2 fixation. On the basis of a compilation of the abundances of the diazotrophic *Trichodesmium*, *Carpenter* [1983] concluded that N_2 fixation in the Pacific Ocean is small and contributes less than 10% to the globally estimated N_2 fixation. However, *Karl et al.* [1992] reported an extensive bloom of *Trichodesmium* near Hawaii. These authors suggested that the nitrogen input by diazotrophs may be an important source of new nitrogen to the euphotic layer near Hawaii. If this is indeed the case of a larger region of the North Pacific, then denitrification must also be higher to apparently keep N^* more or less conservative. If the observed bloom near Hawaii was only

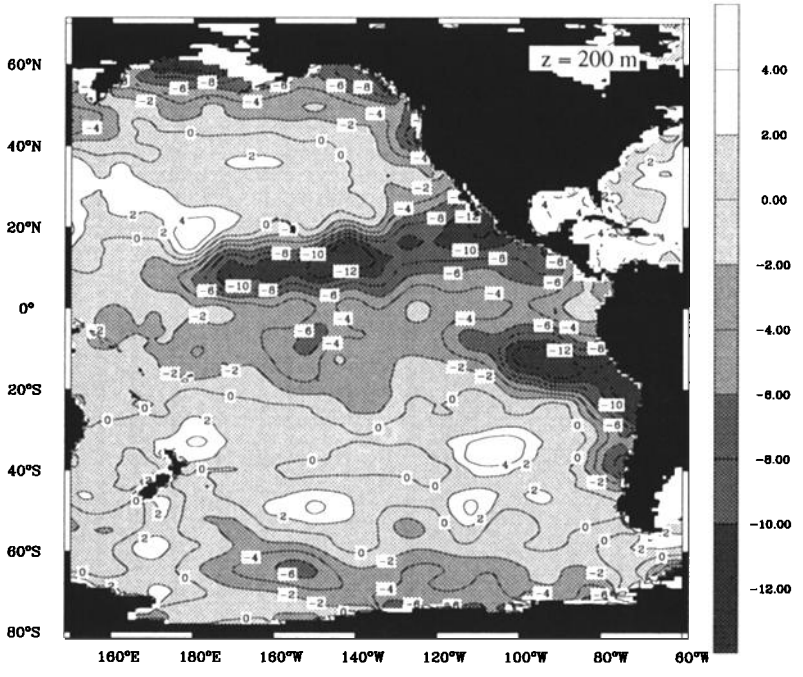

Figure 11. Horizontal distribution of N^* at 200 m in the Pacific Ocean based on the 1° gridded nutrient data of *Conkright et al.* [1994].

an intermittent episode, then both N_2 fixation and denitrification are small in the Pacific outside the regions of strong denitrification.

As in the Indian Ocean, the observed distribution of N^* in the Pacific Ocean supports the utility of the concept of N^*. For large regions in the Pacific, N^* apparently behaves conservatively. N^* becomes negative in the oxygen minimum zones of the eastern Pacific and in some shelf regions where denitrification is known to occur. These low N^* regions at middepth waters are identical to the regions where *Anderson and Sarmiento* [1994] found relatively low $N{:}P$ remineralization ratios. Our more detailed investigation supports their conclusion that denitrification, which they did not take into account in the Pacific, was responsible for these low $N{:}P$ stoichiometric ratios. Owing to the relatively coarse resolution of the Pacific by the GEOSECS data, we are unfortunately not able to draw a more complete picture of the N^* distribution.

Atlantic Ocean

The meridional section of N^* in the Atlantic Ocean (Figure 12) shows a pronounced maximum with values exceeding 3.5 μmol kg^{-1} in the thermocline of the tropical and subtropical North Atlantic. The N^* maximum extends meridionally from the equator to almost 50°N but is vertically well confined between about 100 and 1000 m. Considerably lower values can be found north of this region in the upper 100 m. The N^* concentrations in the North Atlantic Deep Water steadily decrease toward the south from 1.5–2 μmol kg^{-1} to about 0.5–1 μmol kg^{-1}. The thermocline of the southern subtropical gyre shows considerably lower values of N^* than the northern gyre. The Antarctic Intermediate Water (AAIW), the core of which extends northward at a depth of about 1000 m, and the Antarctic Bottom Water exhibit N^* concentrations of –0.5–0.5 μmol kg^{-1}, the typical value found for waters of southern origin in all basins.

The good spatial data coverage in the Atlantic Ocean permit us to prepare maps of objectively analyzed N^* on isopycnal surfaces and therefore to investigate the N^* distribution in the Atlantic Ocean in much more detail than in the other basins. Figure 13 shows N^* on four selected isopycnal surfaces, each representing a typical water mass in the Atlantic Ocean.

The horizontal extent of the N^* maximum within the upper 1000 m of the North Atlantic becomes clearly discernible on the two σ_θ surfaces 26.50 and 27.10 (Figures 13a and 13b). These isopycnals represent the subtropical and the subpolar mode waters [*Kawase and Sarmiento*, 1985]. The maximum on these two isopycnal surfaces is confined to the western North Atlantic, but N^* values above 2.5 μmol kg^{-1} can be found from 10°N to more than 50°N across the entire basin. A persistent feature in all thermocline σ_θ surfaces is an

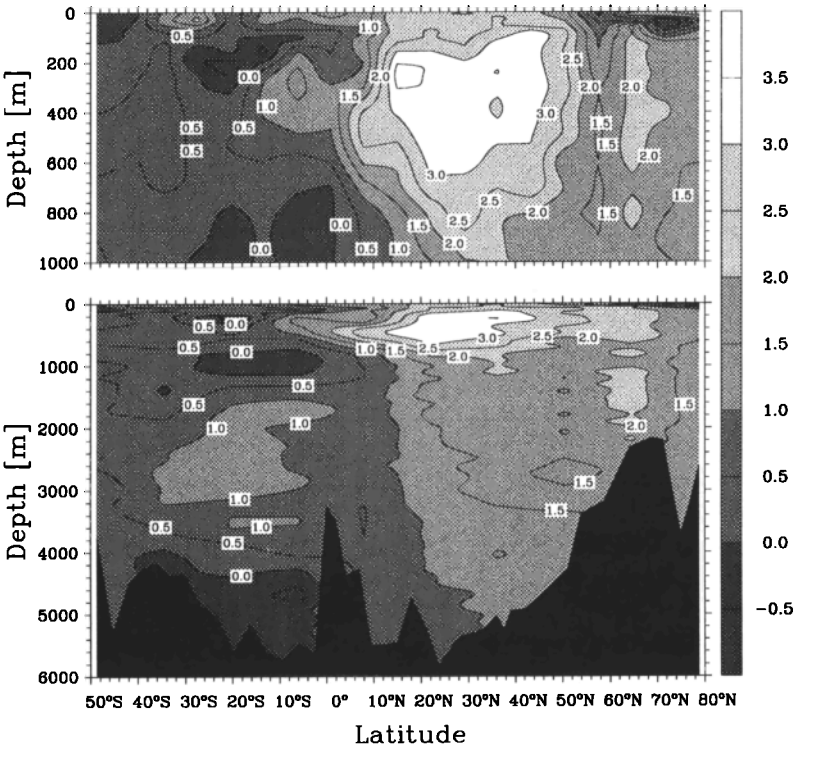

Figure 12. Meridional section of N^* (micromoles per kilogram) in the Atlantic Ocean based on SAVE and TTO nutrient data. See Figure 2 for the station locations.

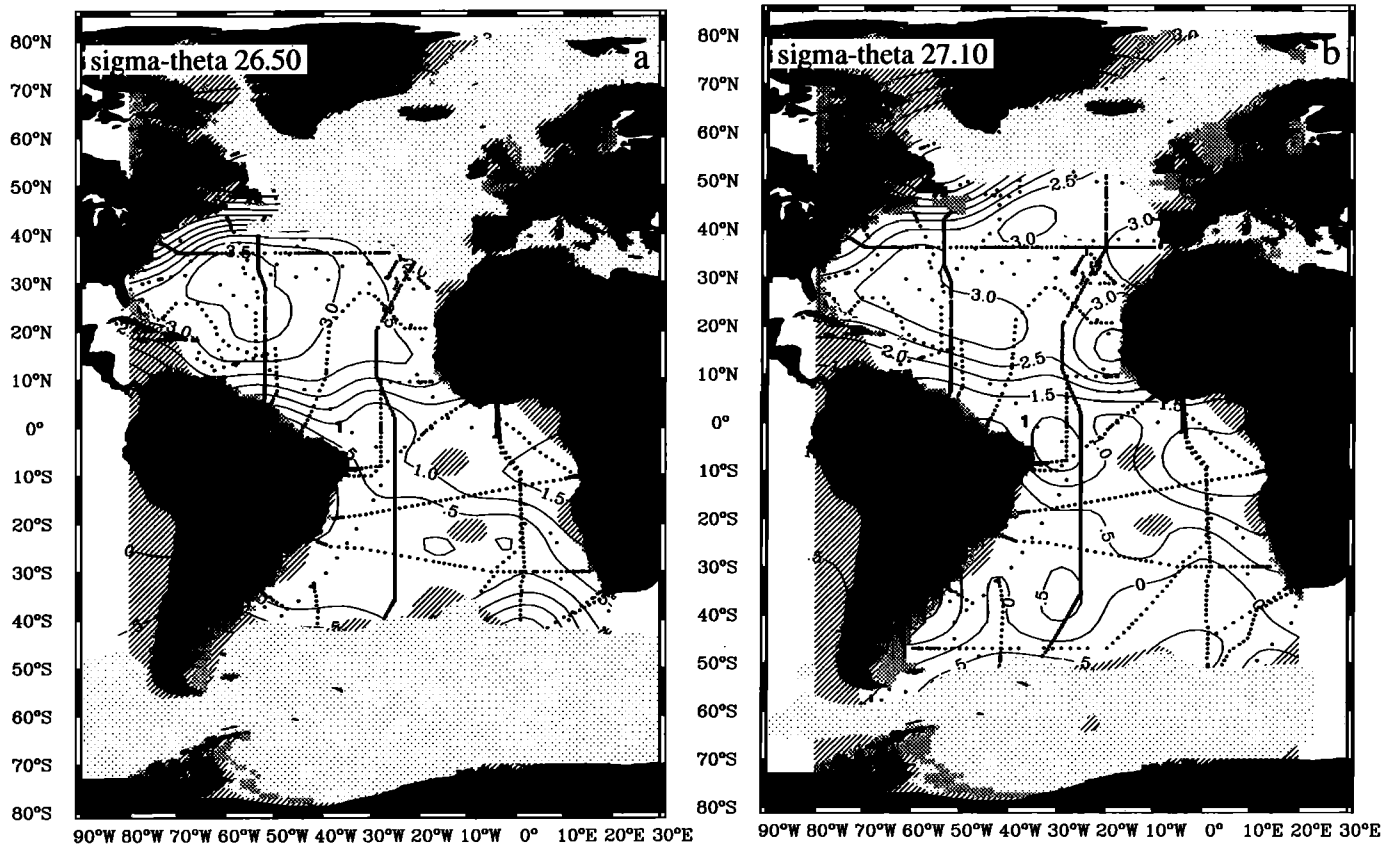

Figure 13. Plots of the objectively analyzed distribution of N^* (micromoles per kilogram) on isopycnal surfaces in the Atlantic Ocean. (a) N^* on the $\sigma_\theta = 26.50$ surface representing the 18° Water in the North Atlantic, (b) N^* on the $\sigma_\theta = 27.10$ surface representing the Subpolar Mode Water, (c) N^* on the $\sigma_2 = 36.40$ surface representing the Antarctic Intermediate Water, and (d) N^* on the $\sigma_2 = 37.00$ surface representing the core of North Atlantic Deep Water. Solid circles denote the stations; stippling denotes areas where the waters of this potential density are not present in winter time (determined from the NOAA NESDIS atlas [*Levitus et al.*, 1994; *Levitus and Boyer*, 1994b]). Cross-hatched areas are regions where the estimated error in objectively analyzed N^* is greater than 0.7 μmol kg^{-1}.

N^* front that runs from northeastern South America across the tropical North Atlantic to the western tip of Africa at about 15°N. This front coincides with the North Equatorial Current and divides the high-salinity northern subtropical gyre waters from equatorial waters of lower salinity [*Kawase and Sarmiento*, 1985]. A second front in N^* is observed along the Gulf Stream separating the slope waters of the North American continent from the gyre waters. The 15°N front is very evident in Figures 14a and 14b where N^* is plotted versus salinity on these two σ_θ surfaces. In the case of σ_θ 26.50 the southern front occurs at a salinity of about 35.75 practical salinity unit (psu), and in the case of σ_θ 27.10 it occurs at a salinity of about 35.00 psu. At high salinities (north of the front), N^* is high and not correlated with salinity. At lower salinities (south of the front), N^* is much lower and tends to correlate with salinity. This indicates a nonconservative behavior of N^* in the North Atlantic subtropical gyre, whereas N^* behaves almost conservatively south of the North Equatorial Current. The influence of the Gulf Stream front in these two figures is almost not discernible since only very few stations are affected.

The σ_2 36.40 surface (Figure 13c) represents the Antarctic Intermediate Waters and the upper outflow waters from the Mediterranean. On this surface the maximum N^* in the North Atlantic has shifted toward the eastern side of the basin. This maximum is now located near the Iberian Peninsula and is associated with the outflow of high-salinity waters of the Mediterranean. This indicates that the Mediterranean is exporting high N^* waters. The relative maximum of N^* in the subtropical North Atlantic extends across the entire basin. The influence of the Mediterranean water and its subsequent mixing with the other water masses is also evident in Figure 14c The Mediterranean end-member has a

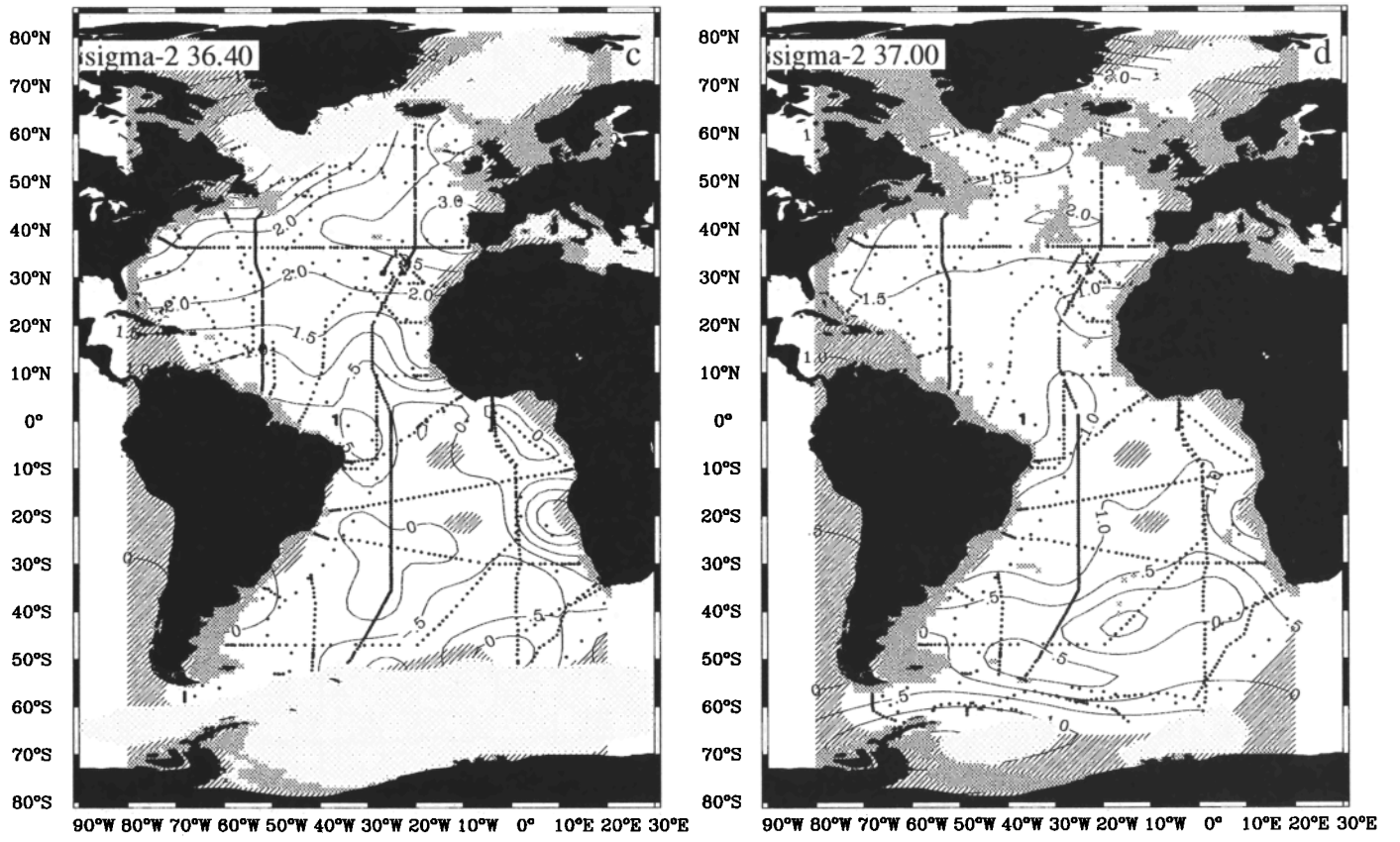

Figure 13. (continued)

salinity of about 37.0 psu and N^* values of about 4 μmol kg^{-1}, the subtropical outcrop end-member has a salinity of about 35.0 psu and N^* concentrations of about 2 μmol kg^{-1}, and the southern end-member (AAIW) has a salinity of about 34.2 psu and N^* concentrations of around 0 μmol kg^{-1}. N^* seems to behave conservatively on this particular isopycnal surface, in contrast to the σ_θ surfaces in the thermocline. The high estimated Mediterranean end-member N^* concentration is supported by high N^* concentrations found throughout the intermediate and deep waters of the Mediterranean at GEOSECS station 404 in the Ionian Sea. The Levantine Intermediate Water which forms the main source for the overflow waters [*Minas et al.*, 1991] has an N^* concentration of about 4 μmol kg^{-1}, in accordance with the estimated end-member concentration of the Mediterranean outflow waters based on the Atlantic Ocean data.

The σ_2 37.00 surface (Figure 13d), which lies within the core of the North Atlantic Deep Water, reveals little variability of N^* in the North Atlantic. More variability can be observed toward the southern outcrop of this surface, where N^* rapidly decreases to values around -0.5 μmol kg^{-1}. A plot of N^* versus salinity shows near conservative behavior of N^* on this isopycnal surface (Figure 14d). Most of the data lie on a mixing line between the northern end-member with a salinity of about 34.96 psu and N^* concentrations of about 2 μmol kg^{-1} and a southern end-member with a salinity of about 34.80 psu and N^* concentrations of about 0 μmol kg^{-1}. For salinities lower than 34.80 psu, N^* shows a large amount of scatter.

In summary, we observe a broad maximum of N^* within the thermocline of the subtropical North Atlantic, where N^* does not behave conservatively, and an almost conservative behavior for most of the rest of the Atlantic Ocean. Additionally, there is an indication of low values near the North American shelf and the export of high N^* concentrations from the Mediterranean.

We believe that the extensive maximum in the North Atlantic thermocline is due to the remineralization of nitrogen-rich organic matter from diazotrophic organisms. Is this consistent with our knowledge about the role of N_2 fixation in the Atlantic Ocean?

Carpenter [1983] summarized all available historical observations of *Trichodesmium* blooms in the Atlantic Ocean and found persistently high trichome concentrations during all seasons, especially in the Caribbean Sea and in the western tropical North Atlantic. Farther north the estimated trichome concentrations varied strongly with seasons. These observations are confirmed by *Carpenter and Romans* [1991] who reported

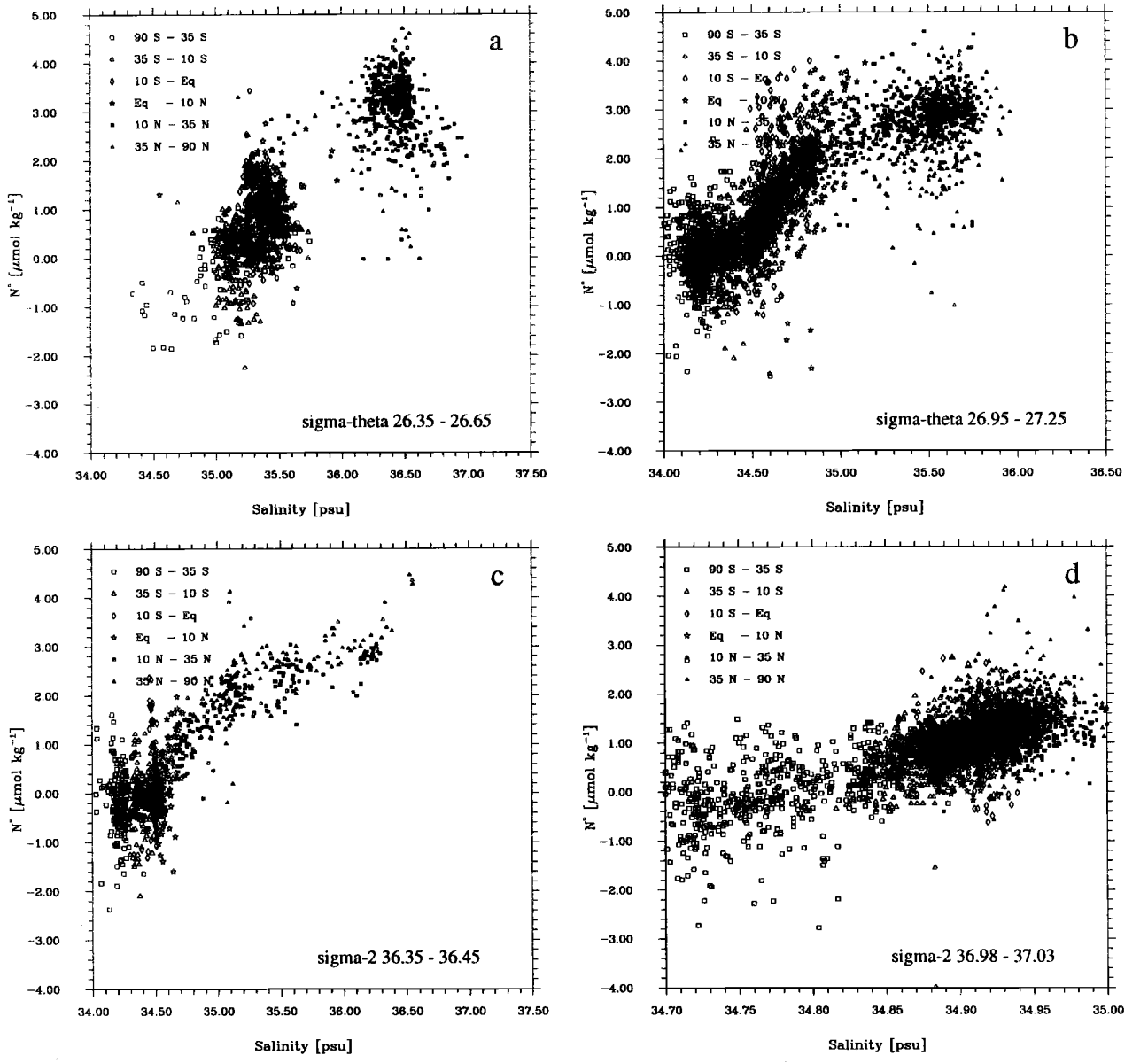

Figure 14. Plots of N^* versus salinity on isopycnal surface intervals in the Atlantic Ocean. (a) σ_θ surface interval 26.35–26.65, (b) σ_θ surface interval 26.95–27.25, (c) σ_2 surface interval 36.35–36.45, and (d) σ_2 surface interval 36.98–37.03.

high concentrations of *Trichodesmium* colonies on a north-south transect in the tropical North Atlantic. They concluded that *Trichodesmium* plays a central role in fixation of carbon and the introduction of new nitrogen to the euphotic zone in this region, a conclusion that is supported by the few reported measurements of N_2 fixation rates in this region [*Goering et al.*, 1966; *Carpenter and Price*, 1977]. Thus our observation of a broad N^* maximum in the western tropical and subtropical North Atlantic is entirely consistent with these observations. Our data even indicate that significant N_2 fixation may not be limited only to the western tropical North Atlantic but leaves its imprint also in the central regions of the subtropical North Atlantic.

Owing to lack of sufficient data, *Carpenter* [1983] was not able to estimate population sizes of *Trichodesmium* in the Mediterranean and therefore did not calculate a N_2 fixation rate for this basin. *Béthoux and Copin-Montégut* [1986] and *Béthoux et al.* [1992], however, concluded from a study of the nitrogen balance in the Mediterranean Sea that nitrogen fixation must contribute significantly to this balance. Such a high N_2 fixation rate is consistent with our observations of high N^* values in the Mediterranean.

The continental shelf sediments along the eastern coast of North America are known to be sites of sedimentary denitrification [*Christensen et al.*, 1987b; *Seitzinger and Giblin*, 1996]. On the basis of simple model of coupled nitrification/denitrification, *Seitzinger and Giblin* [1996] estimated that approximately 30% of the total calculated sedimentary denitrification in the Atlantic Ocean north of the equator occurs on the shelfs of the eastern coast of North America. Thus the strong N^* front associated with the Gulf Stream and the much lower values in the slope waters are the geochemical signature of the denitrification process in the shelf sediments. We find, however, no clear indication of sedimentary denitrification in the other shelf regions of the North Atlantic Ocean, although according to *Seitzinger and Giblin* [1996] the remaining 70% of their estimated sedimentary denitrification is occuring there. This is quite probably due to the overwhelming effect of the N_2 fixation signal, which makes the Atlantic Ocean a net global source of fixed nitrogen.

Nitrogen Fixation in the Tropical to Subtropical North Atlantic

The distribution of N^* in combination with transient tracers can be used to infer rates of N_2 fixation and/or denitrification. We make advantage of the fact that these two processes are often spatially separated, so that a nonconservative behavior of N^* can be interpreted as being solely due to just one of these processes. This is the case in the tropical to subtropical North Atlantic, where we attribute the observed N^* maximum to the integrated effect of nitrogen fixation. We attempt here to estimate the rate of nitrogen fixation in this region using our N^* data together with concurrent transient tracer observations.

We assume that transport in the interior of the ocean occurs primarily along isopycnal surfaces and that mixing on any particular surface can be described by either a one or a two end-member mixing model. Let us first consider the two end-member case (see Figure 15). The first end-member has properties T_1, N_1^*, τ_1, and the second has T_2, N_2^*, τ_2, and T stands for any suitable conservative tracer (e.g., salinity or PO_4^* [*Broecker et al.*, 1991]), and τ stands for an idealized age tracer. Following *Thiele and Sarmiento* [1990] and a similar suggestion by *Siegenthaler* [1982], the continuity equation for this age tracer is given by

$$\Gamma(\tau) = 1, \tag{18}$$

with the boundary condition $\tau(\text{outcrop}) = 0$. For any water parcel at an intermediate location (i) on this surface the concentrations can be written as follows [*Anderson and Sarmiento*, 1994]:

$$1 = f_1^i + f_2^i, \tag{19}$$

$$T_{\text{obs}}^i = f_1^i\, T_1 + f_2^i\, T_2, \tag{20}$$

$$N_{\text{obs}}^* = f_1^i\, N_1^* + f_2^i\, N_2^* + \Delta N_i^*, \tag{21}$$

$$\tau_{\text{obs}} = f_1^i\, \tau_1 + f_2^i\, \tau_2 + \Delta\tau_i, \tag{22}$$

where subscript obs stands for an observation and f stands for end-member fraction. ΔN_i^* is the integrated contribution of denitrification and/or N_2 fixation on N^* over the time $\Delta\tau_i$ since the water parcels left the end-member locations at time τ_1 and τ_2, respectively,

$$\Delta N_i^* = \int_0^{\Delta\tau_i} \left(J_{\text{denitr}}(N) + 0.76\, J_{\text{N-rich nitr}}(N)\right) dt. \tag{23}$$

Suppose we are able to estimate the ideal ages, τ_1, τ_2, and τ_{obs}, then we can calculate the average denitrification and/or N_2 fixation rates that occurred since the water parcels left the end-member locations. Thus

$$\overline{J_{\text{denitr}}(N) + 0.76\, J_{\text{N-rich nitr}}}\Big|_{\Delta\tau_i} = \frac{\Delta N_i^*}{\Delta\tau_i}. \tag{24}$$

If the source minus sink term of denitrification and/or N_2 fixation are nearly constant over the region under consideration, then the slope of a linear regression in a plot of ΔN_i^* versus $\Delta\tau_i$ would yield the average rate of the sum of these processes. Our technique here is roughly equivalent to previous methods used for estimating oxygen utilization rates in the Atlantic [*Jenkins*, 1987; *Broecker et al.*, 1991]

In the case of single end-member mixing, (19) - (22) simplify to

$$N_{\text{obs}}^* = N_1^* + \Delta N_i^*\,, \tag{25}$$

$$\tau_{\text{obs}} = \tau_1 + \Delta\tau_i\,. \tag{26}$$

Following *Jenkins* [1987], we approximate the ideal water age τ by the tritium-helium-3 age ($\tau_{\text{T/He}}$) calculated from concurrent tritium (^{3}H) and helium-3 (^{3}He) observations by

$$\tau_{\text{T/He}} = \lambda^{-1} \ln\left(1 + \frac{[^3\text{He}]}{[^3\text{H}]}\right). \tag{27}$$

The brackets denote the concentrations in appropriate units (TU), and λ is the tritium decay constant (1.77×10^{-9} s^{-1}). The tritium-helium-3 age ($\tau_{T/He}$) is not equal to the ideal age (τ) since mixing affects $\tau_{\text{T/He}}$ in a nonlinear way by making it younger compared to τ [*Jenkins*, 1987]. *Jenkins and Wallace* [1992] investigated the deviations of $\tau_{\text{T/He}}$ from age ideality both directly and by numerical model simulations (based on the work by *Thiele and Sarmiento* [1990]). They concluded that throughout much of the subtropical gyre, the tritium-helium-3 age differs from the ideal age by 10% or less. This is small in comparison with the uncertainties associated with the calculation of N^*, and

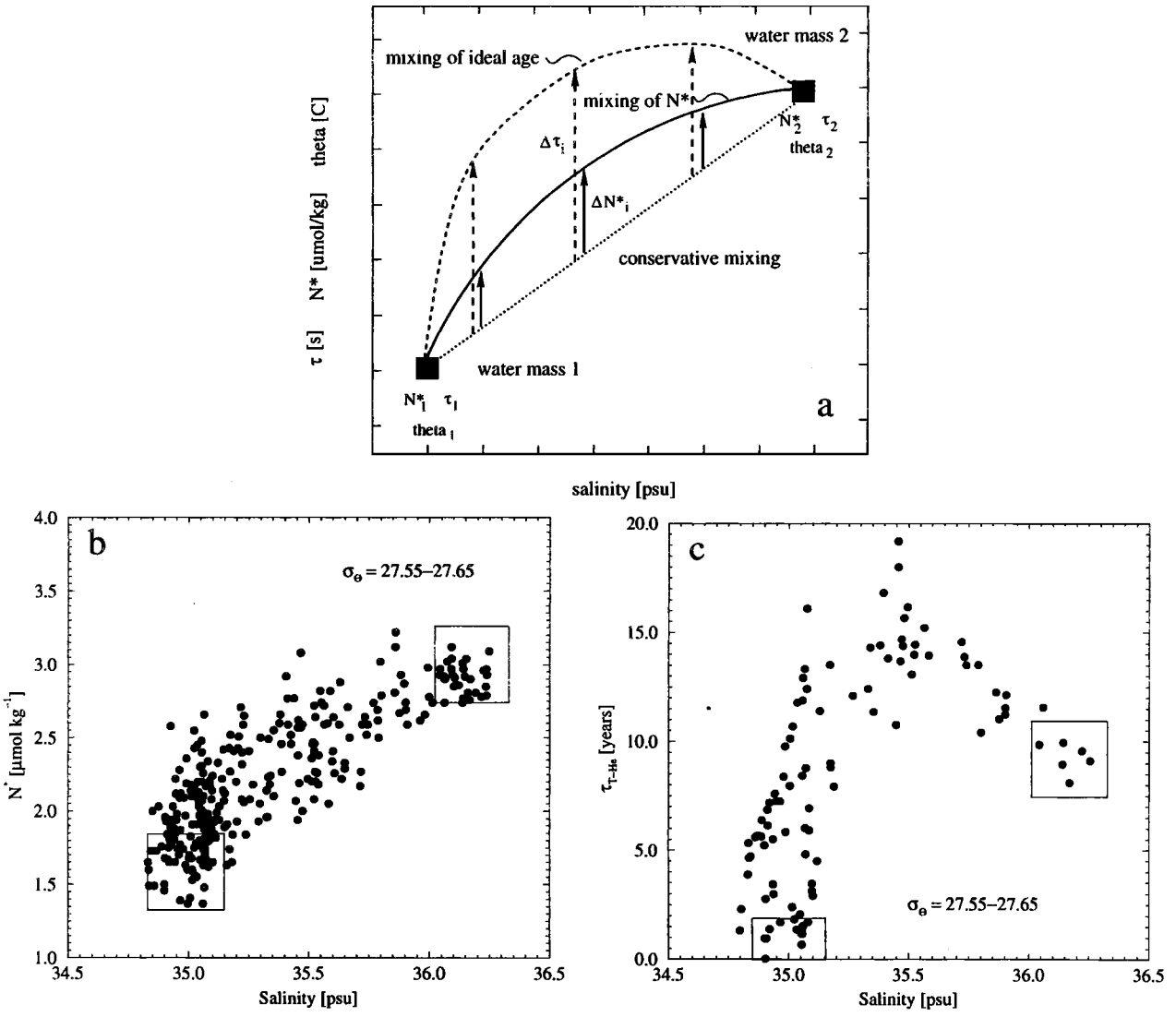

Figure 15. (a) N^*, potential temperature (theta), and ideal age (τ) versus salinity in a hypothetical two end-member mixing system. In this example, nitrification of nitrogen-rich organic matter from diazotrophic organisms causes an upward bow of N^* from the conservative mixing line between the two end-member water masses (ΔN^*_i). Owing to the aging of the waters as they are transported away from the end-members the ideal age τ also shows such an upward bow. The age of a water parcel since it left the end-member locations is shown by $\Delta\tau_i$. (b) N^* and (c) tritium-helium-3 age (τ_{T-He}) versus salinity on the isopycnal surface interval 27.55-27.65 in the North Atlantic. The end-members on this surface interval (boxes) are the North Atlantic subpolar outcrop waters on the left side (salinity of about 35.0 psu) and the Mediterranean overflow waters on the right side (salinity of about 36.2 psu). N^* behaves almost conservatively on this surface interval.

we will therefore neglect the difference between $\tau_{T/He}$ and τ.

We use tritium and helium-3 observations from the TTO NAS (1981) and the Atlantis 109 (1981) cruises to calculate $\tau_{T/He}$. These data were obtained by the Woods Hole Oceanographic Institution Helium Isotope Laboratory. We determined ΔN^* versus $\Delta\tau$ on a total of thirteen σ_θ surface intervals in the upper 1000 m (see Table 1). All stations lying poleward of the wintertime outcrop of these surfaces based on the NOAA NESDIS atlas [*Levitus et al.*, 1994; *Levitus and Boyer*, 1994b] were excluded. We assumed single end-member mixing for the σ_θ intervals between 25.45 and 27.35 and two end-member mixing for the three intervals between σ_θ 27.35 and 27.65, where the overflow water from the Mediterranean is forming a second distinct end-member (see Figures 15b and 15c). The end-member concentrations that we chose are also shown in Table 1. In the

Table 1. Estimated Values of the Rate of Change of N^* on Isopycnal Surfaces in the North Atlantic

Potential Density		End-Member Composition									
Midval	Interval	N_1^*, μmol kg^{-1}	N_2^*, μmol kg^{-1}	S_1, psu	S_2, psu	τ_1, yr	τ_2, yr	N_{obs}, #	slope,[a] μmol kg^{-1} yr^{-1}	σ_{slope},[b] μmol kg^{-1} yr^{-1}	r^2
25.60	25.45–25.75	2.38				0		6	0.071	0.025	0.66
25.90	25.75–26.05	1.88				0		10	0.408	0.101	0.67
26.20	26.05–26.30	2.17				0		8	0.351	0.075	0.85
26.40	26.30–26.50	2.68				0		36	0.139	0.022	0.74
26.60	26.50–26.70	2.45				0		41	0.119	0.022	0.66
26.80	26.70–26.90	2.26				0		58	0.117	0.012	0.71
27.00	26.90–27.05	2.49				0		64	0.063	0.014	0.38
27.10	27.05–27.15	2.55				0		54	0.028	0.013	0.16
27.20	27.15–27.25	2.65				0		45	0.017	0.014	0.05
27.30	27.25–27.35	2.08				0		47	0.039	0.016	0.15
27.40	27.35–27.45	1.50	3.00	34.9	36.0	0	8	71	0.000	0.008	0.00
27.50	27.45–27.55	1.20	3.00	34.8	36.0	0	9	67	-0.001	0.009	0.00
27.60	27.55–27.65	1.60	3.00	35.0	36.2	0	9	103	-0.013	0.008	0.03

[a]Slope of the linear regression of the form $\Delta N^* = a\,\Delta\tau + b$ (see equation (24)).
[b]1σ uncertainty of the slope a of this regression.

case of two end-member mixing the end-member concentrations have been determined from plots of N^* and τ versus salinity.

We find distinct patterns of ΔN^* versus $\Delta\tau$ on all isopycnal surface intervals (Figure 16). On the surfaces between σ_θ 25.45 and σ_θ 27.15, ΔN^* is significantly positively correlated with $\Delta\tau$, whereas on the deeper surface intervals (σ_θ 27.15-27.65) no significant correlation exists. Linear regressions of the form $\Delta N^* = a\,\Delta\tau + b$ were calculated on all surface intervals, and the resulting slopes a are listed in Table 1 together with their 1σ uncertainty. The observed nonconservative behavior of N^* is due to the combined effect of denitrification and the nitrification of nitrogen-rich organic matter from diazotrophs. Since the waters in the main thermocline of the North Atlantic are well oxygenated, we consider denitrification, even in anoxic microenvironments, to be negligible. If denitrification in microenvironments turns out to be more important, then our estimate of nitrification of N-rich organic matter will be biased on the low side. We can therefore calculate the average source strength $\overline{J_{\text{N-rich nitr}}}$ by dividing the slope by 0.76 (see equation (24)).

High values of $\overline{J_{\text{N-rich nitr}}}$ are found on the σ_θ surface intervals from 25.75–26.30 (see Table 2 and Figure 17). $\overline{J_{\text{N-rich nitr}}}$ is nearly constant at about 0.2 μmol kg^{-1} yr^{-1} in the σ_θ range between 26.30 and 26.90. Below σ_θ 26.90, $\overline{J_{\text{N-rich nitr}}}$ decreases to values not significantly different from zero.

In order to transform these values into an areal estimate, we determined the volume of each isopycnal layer in the region from 10°N to 50°N and 90°W to 10°W using the NOAA NESDIS atlas [*Levitus et al.*, 1994; *Levitus and Boyer*, 1994b]. Multiplying $J_{\text{N-rich nitr}}$ for each isopycnal layer with the volume of that layer results in the volume integrated source strength of the nitrification of organic material from diazotrophs. This can then be equated to the total amount of pelagic nitrogen fixation in the investigated region in the North Atlantic.

We find a total N_2 fixation of about $(23 \pm 2) \times 10^{11}$ mol N yr^{-1} over the investigated region in the North Atlantic. The uncertainty is based on quadratic error addition of the uncertainties calculated for each isopycnal surface layer. However, the N:P ratio in N-rich organic matter of diazotrophic organisms ($r^{N:P}_{\text{N-rich nitr}}$) is very uncertain. Figure 18 shows that the estimated N_2 fixation is not strongly dependent on the chosen value of $r^{N:P}_{\text{N-rich nitr}}$. Changing $r^{N:P}_{\text{N-rich nitr}}$ by 50% from our standard value of 125 results only in a change of 4–17%. The uncertainty of our estimate of N_2 fixation should therefore not be much larger than about 5×10^{11} mol N yr^{-1}.

We have neglected so far the contribution of other processes that have the potential to alter N^*. First, we did not take into account the contribution of the atmospheric deposition in the subtropical North Atlantic [*Fanning*, 1989], although the deposition rates are relatively high, and the atmospheric input has N:P ratios well above 100:1 [*Duce*, 1986]. *Duce et al.* [1991] estimated a total N deposition flux over the North Atlantic of 156 mg N m^{-2} yr^{-1}. This is equal to a deposition of 3.1×10^{11} mol N yr^{-1} over the tropical and subtropical North Atlantic (27.8×10^{12} m^2) or about 13% of our estimated N_2 fixation. We therefore reduce our estimate of pelagic N_2 fixation by this amount to 20×10^{11} mol N yr^{-1}. Second, it is possible that a differential flux

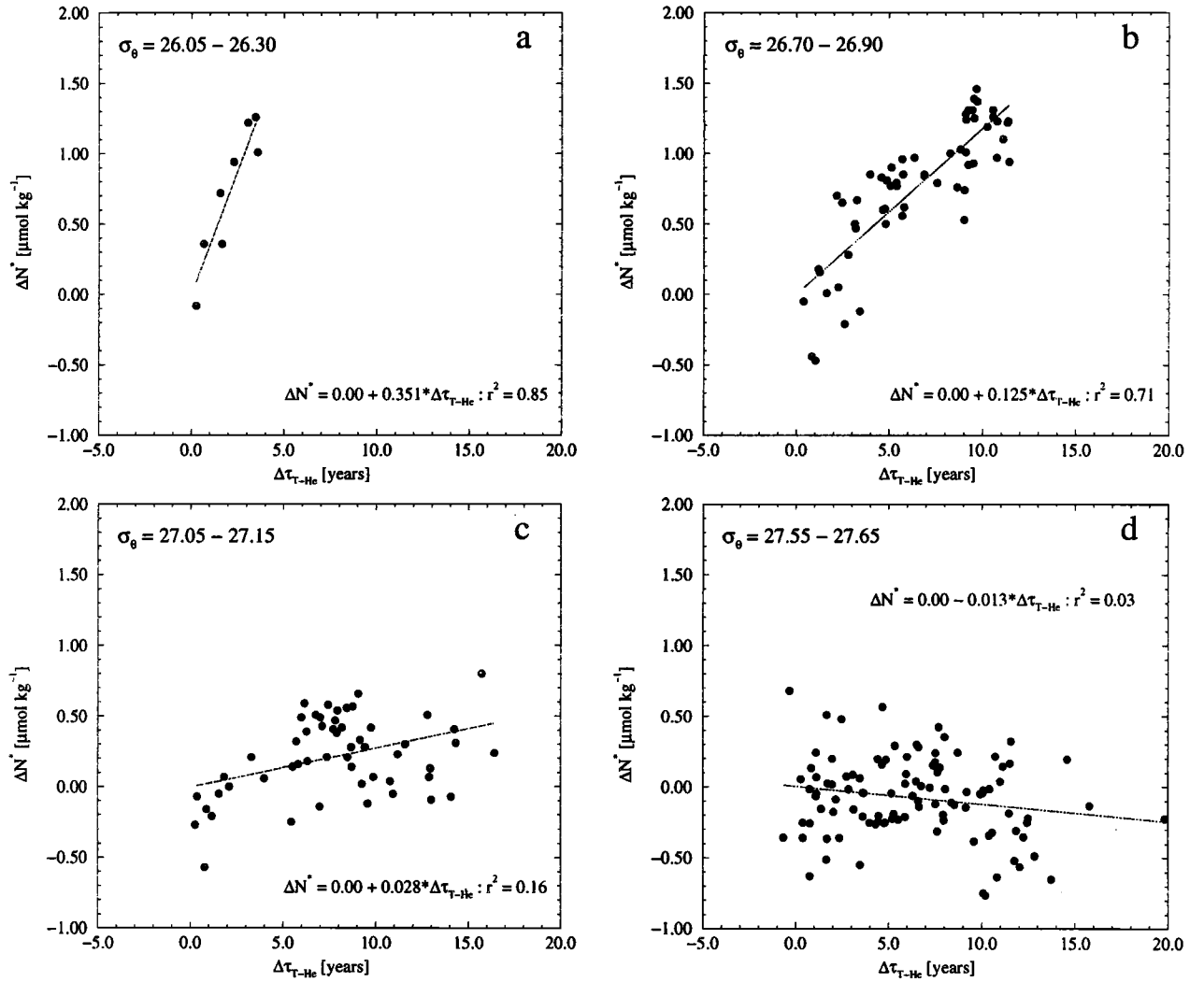

Figure 16. Plot of ΔN^* versus $\Delta\tau_{THe}$ on the σ_θ surface intervals (a) 26.05-26.30, (b) 26.70-26.90, (c) 27.05-27.15, and (d) 27.55-27.65. Single end-member mixing has been assumed for the first three surface intervals, whereas two end-member mixing has been assumed for (d). See Table 1 for further details. Also shown are the results of linear regressions.

or lability of dissolved organic nitrogen (DON) relative to dissolved organic phosphate (DOP) creates a non-conservative behavior of N^*. This possibility is very difficult to constrain, largely because DON and DOP are rarely measured. However, *Michaels et al.* [1996] argue that dissolved organic matter is very unlikely responsible for the observed pattern of N^* in the North Atlantic because it must have very unlikely characteristics to create the mid gyre thermocline maximum in N^*. However, until adequate surveys of DON and DOP are performed, a dissolved organic source cannot definitively be ruled out. Third, we have neglected the potential of selective uptake of nutrients by organisms which are capable of regulating their buoyancy. Such a selective uptake has been proposed, for example, for *Trichodesmium* [*Karl et al.*, 1992] (see also below). The selective uptake of phosphate would mostly occur at the top of nutricline, which lies between 100 and 200 m depth near Bermuda [*Michaels and Knap*, 1996]. This would lead to an increase of N^* at these depths, and we would therefore overestimate the remineralization rate of nitrogen-rich organic matter there. We attempt to estimate the maximum effect of this selective uptake by assuming that the entire phosphate requirement for our estimated annual N_2 fixation is obtained between 100 and 200 m and none of the produced nitrogen-rich organic matter is remineralized in this depth range. Our estimated N_2 fixation in the tropical and subtropical North Atlantic requires about 6×10^{-4} mol m^{-2} yr^{-1} phosphate. This leads to a concentration change of about 6×10^{-6} mol m^{-3} yr^{-1} in this depth interval, and is equivalent to a change in N^* of about 8×10^{-5} mol

Table 2. Summary of the Estimated Rates of Nitrification of Nitrogen-Rich Organic Material from Diazotrophic Organisms on Isopycnal Surfaces in the North Atlantic

Potential Density	$d\Delta N^*/d\Delta\tau$, μmol kg^{-1} yr^{-1}	$\sigma_{d\Delta N^*/d\Delta\tau}$, μmol kg^{-1} yr^{-1}	$\overline{J_{\text{N-rich nitr}}}$,[a] mmol m^{-3} yr^{-1}	σ, mmol m^{-3} yr^{-1}	Volume,[b] 10^{15}m^3	$\int_V \overline{J_{\text{N-rich nitr}}} dV$,[c] 10^{11}mol yr^{-1}	σ, 10^{11}mol yr^{-1}
25.60	0.071	0.025	0.096	0.034	0.41	0.39	0.14
25.90	0.408	0.101	0.551	0.136	0.66	3.63	0.90
26.20	0.351	0.075	0.474	0.101	0.91	4.31	0.92
26.40	0.139	0.022	0.188	0.030	1.50	2.82	0.45
26.60	0.119	0.022	0.161	0.030	2.14	3.44	0.64
26.80	0.117	0.012	0.158	0.016	2.68	4.24	0.43
27.00	0.063	0.014	0.085	0.019	2.63	2.24	0.50
27.10	0.028	0.013	0.038	0.018	2.15	0.81	0.38
27.20	0.017	0.014	0.023	0.019	2.32	0.53	0.44
27.30	0.039	0.016	0.052	0.021	2.46	1.30	0.53
27.40	0.000	0.008	0.000	0.011	2.61	0.00	0.28
27.50	-0.001	0.009	-0.001	0.012	2.83	-0.04	0.34
27.60	-0.013	0.008	-0.017	0.011	3.46	-0.61	0.38
Total					26.76	23.07	1.92

[a]Calculated from $d\Delta N^*/d\Delta\tau$ under the assumption that no denitrification occurs.
[b]Estimated volume of these isopycnal layers in the region from 10°N to 50°N and from 90°W to 10°W.
[c]Calculated by multiplying V with $\overline{J_{\text{N-rich nitr}}}$.

m^{-3} yr^{-1}. We would erroneously interpret this change in N^* to be due to the remineralization of nitrogen-rich organic matter from diazotrophs and infer an apparent vertically integrated value over this depth range of 0.008 mol m^{-2} yr^{-1}. This is equivalent to an apparent N_2 fixation of 0.011 mol m^{-2} yr^{-1}. Thus we overestimate in our example the N_2 fixation by about 15% due to the neglect of the selective uptake of nutrients. This is a maximum value and the "true" overestimate is very likely to be smaller because a part of the nitrogen-rich organic matter of diazotrophs is remineralized in between 100 and 200 m and not all required P is selectively taken up at depth. We therefore conclude that the possible selective uptake of nutrients should not not pose a serious problem in our calculations but acknowledge that we cannot quantify the effect more accurately.

How does our estimate of nitrogen fixation of 20×10^{11} mol N yr^{-1} compare with previous estimates of pelagic nitrogen fixation in the North Atlantic or in the global ocean? Table 3 shows a summary of estimates of pelagic nitrogen fixation in the (North) Atlantic and the global oceans. Our N^*-based estimate is an order of magnitude larger than the original estimate of *Capone and Carpenter* [1982]. It is, however, less than half as large as a recent estimate by *Michaels et al.* [1996] which is based on the distribution of N^* at the U.S. Joint Global Ocean Flux Study (JGOFS) Bermuda Atlantic Time-series Study (BATS) site near Bermuda and a simple tritium box model [*Sarmiento*, 1983; *Jenkins*, 1980] for deriving rates. The major reason for the discrepancy between our results and those of *Michaels et al.* [1996] is due to the selection of different end-members. We regard their estimate to be quite likely an overestimate because they chose much lower N^* end-members at the outcrops than can be supported by the N^* distribution in the North Atlantic (see Figures 13a-13c). In the potential density range σ_θ 26.30 to σ_θ 27.25 the N^* end-members of *Michaels et al.* [1996] are on average 1.8 ± 0.4 μmol kg^{-1} lower than ours. This difference is more than 50% of the change of N^* between the outcrop and the value at BATS. Since they use only this change in N^* to calculate the N_2 fixation, the end-member choice is extremely critical. Our estimate, on the other hand, does not depend on the choice of the appropriate end-member but depends rather on the slope defined by the data from many more stations. Additional differences arise because of the different techniques used to estimate the ventilation timescales for the isopycnal layers.

Our estimate of nitrogen fixation in the tropical and subtropical North Atlantic is about 6 times larger than the global estimate of *Capone and Carpenter* [1982] and about 3 times larger than the global estimate of *Carpenter and Capone* [1992] where the contribution of *Trichodesmium* blooms have been taken into account. It is, however, consistent with the recent tentative estimate of *Galloway et al.* [1995] which extrapolated the measurements of *Carpenter and Romans* [1991] in the Atlantic Ocean to the world oceans. Our result suggests that marine pelagic nitrogen fixation is indeed significantly higher than previously thought.

The estimate of 20×10^{11} mol N yr^{-1} is equivalent to a mean nitrogen fixation rate over the tropical and sub-

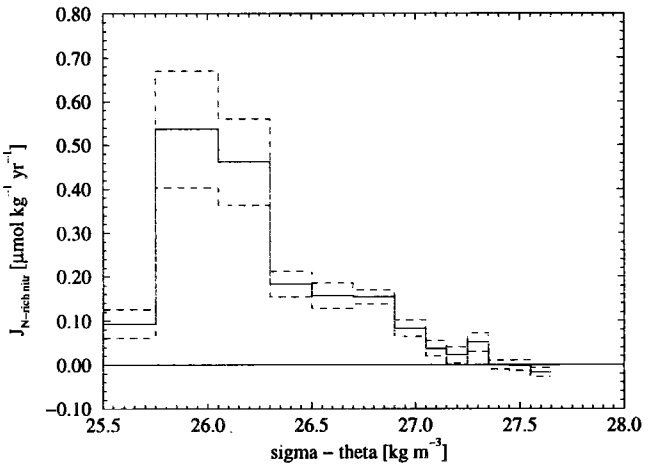

Figure 17. Plot of the calculated source strength of nitrification of nitrogen-rich organic material originating from diazotrophic organisms ($J_{\text{N-rich nitr}}$) on the investigated sigma-theta surface intervals in the North Atlantic. The dashed lines represent the values at $\pm 1\sigma$ of the estimates.

tropical North Atlantic Ocean (27.8×10^{12} m^2) of 0.072 mol N m^{-2} yr^{-1}. This average over large temporal and spatial scales is of the same order of magnitude as the highest older reported areal fixation rates [*Carpenter*, 1983]. It is, however, smaller than the estimate by *Carpenter and Romans* [1991], who found an areal fixation rate of about 0.77 mol N m^{-2} yr^{-1} in the Caribbean and tropical North Atlantic. *Béthoux and Copin-Montégut* [1986] estimated a very similar areal N_2 fixation rate of 0.04–0.06 mol N m^2 yr^{-1} in the Mediterranean Sea based on a nitrogen budget for this basin.

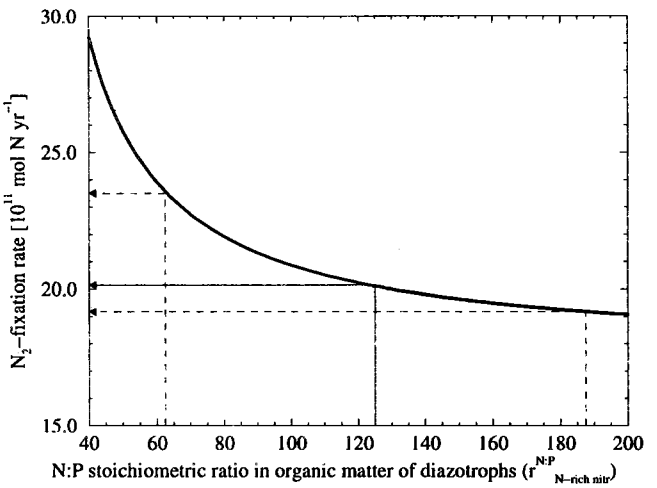

Figure 18. Plot of the estimated N_2 fixation rate in the subtropical North Atlantic (10°N–50°N) as a function of the $N{:}P$ stoichiometric ratio of N-rich organic matter of diazotrophs, $r^{N:P}_{\text{N-rich nitr}}$. We have chosen a value of 125 for $r^{N:P}_{\text{N-rich nitr}}$ which results in an estimated N_2 fixation of 20×10^{11} mol N yr^{-1} over this region. Changing $r^{N:P}_{\text{N-rich nitr}}$ by 50% results only in a change of $(1-4) \times 10^{11}$ mol N yr^{-1} (5–20%) for the estimated N_2 fixation. Note that this estimate here already contains the 3×10^{11} mol N yr^{-1} reduction because of the influence of atmospheric deposition on N^* (see text).

The addition of fixed nitrogen to the ocean by N_2 fixation can also be compared with the nutrient requirements of the phytoplankton in the mixed layer at station BATS in the northwestern Sargasso Sea during the summer season. *Marchal et al.* [1996] calculated a net community production of about 0.51–0.86 mol C m^{-2} in the mixed layer between April and October based on a mixed layer model and observations of the inorganic carbon system. This net community production, which is equivalent to an N requirement of about 0.070–0.118 mol N m^{-2} during this 7 months period assuming a $C{:}N$ stoichiometry of 117:16 [*Anderson and Sarmiento*, 1994], occurs in the absence of measurable nutrients [*Michaels and Knap*, 1996; *Michaels et al.*, 1994b]. Vertical transport from below is insufficient since the nutricline is more than 30 m below the maximum depth of the mixed layer during this period [*Marchal et al.*, 1996]. Atmospheric N deposition may contribute significantly over short episodes [*Owens et al.*, 1992] but is much too low for a sufficient contribution over the entire summer period [*Michaels et al.*, 1993]. It has been suggested that nitrogen fixation could be responsible

Table 3. Summary of Estimated Nitrogen Fixation Rates in the North Atlantic Ocean and in the Global Oceans

Study	N_2 Fixation Rate	
	10^{11} mol N yr^{-1}	Tg N yr^{-1}
Atlantic Ocean		
Capone and Carpenter [1982][a]	0.9	1.3
Michaels et al. [1996][b]	37–64	52–90
this study [c]	20	28
Global Ocean		
Capone and Carpenter [1982][a]	3.4	5
Carpenter and Capone [1992][d]	7.3	10
Galloway et al. [1995][e]	29–143	40–200

[a] Based on a global compilation of nonbloom *Trichodesmium* abundance and average per trichome nitrogen fixation rate.

[b] Based on vertical N^* distribution at Joint Global Ocean Flux Study (JGOFS) station BATS near Bermuda and the tritium box model of *Sarmiento* [1983].

[c] North Atlantic ocean from 10°N to 50°N and 90°W to 10°W.

[d] As a but including contribution of blooms.

[e] Extrapolation of average fixation rate found by *Carpenter and Romans* [1991] in the Caribbean and tropical North Atlantic.

for explaining this inconsistency [*Michaels et al.*, 1994a; *Marchal et al.*, 1996], but available observations of the abundance of diazotrophs and in situ measurements of nitrogen fixation rates do not support this [*Carpenter and Price*, 1977; *Duce*, 1986; *Carpenter et al.*, 1987]. In contrast, our large-scale estimate of nitrogen fixation in the tropical to subtropical North Atlantic of 0.072 mol N m^{-2} yr^{-1} is sufficient to contribute almost all the nitrogen that is required for sustaining such a net community production in the mixed layer during the summer season, under the assumption that the yearly nitrogen fixation occurs during these 210 days.

But how are these organisms capable of getting the required phosphate? *Karl et al.* [1992] proposed a P transport model, in which *Trichodesmium* cells / trichomes transfer P between the nutricline and the ocean's surface by active regulation of their buoyancy. The cycle starts at depth, where *Trichodesmium* takes up P in excess of its demand, then ascends to the surface ocean, where it fixes nitrogen as long as the P storage is sufficient. When the internal P stock is exhausted, *Trichodesmium* becomes negatively buoyant and descends down to the nutricline, where a new cycle starts. If the conclusion that N_2 fixation makes a major contribution to the nitrogen cycle in the mixed layer at BATS is correct, this would have far reaching effects because one would have to reshape the existing biological paradigms about the controls of the seasonal cycle of primary production in this oligotrophic region.

Measurements of $\delta^{15}N$ of organic matter offer the potential to test our hypothesis that N_2 fixation contributes significantly to the nitrogen cycle in the mixed layer in the subtropical to tropical North Atlantic [*Altabet and McCarthy*, 1985]. This is because nitrogen fixation produces organic matter with a $\delta^{15}N$ of around −2 to −1‰ [*Hoering and Ford*, 1960], whereas the average $\delta^{15}N$ of nitrate is about 6‰ [*Cline and Kaplan*, 1975]. Support for the importance of nitrogen fixation in the subtropical to tropical North Atlantic is provided by the relatively low $\delta^{15}N$ of nitrate in the 18°Water (3.5‰) [*Altabet*, 1988] compared to the oceanic average (6‰) and by the low $\delta^{15}N$ of suspended particulate organic nitrogen (PON) in the euphotic layer (−0.2 ‰) [*Altabet*, 1988]. The observed decrease of $\delta^{15}N$ of PON with depth is also consistent, but other causes could be responsible (M. A. Altabet, personal communication, 1996). On the other hand, the $\delta^{15}N$ of sinking PON measured by sediment traps at 100 m in the Sargasso Sea is about 3.5‰, which suggests that nitrate below the euphotic zone is the major source of nitrogen for the particles leaving the euphotic zone and that nitrogen fixation is small [*Altabet*, 1988]. The inconsistencies between these different measurements may be explained by a number of factors such as fractionation of ^{15}N by macrozooplankton [*Altabet*, 1988], unsampled episodic events, problems with swimmer removal (zooplankton that actively enter the traps) and hydrodynamic biases [*Michaels et al.*, 1994a; *Buesseler et al.*, 1994]. Furthermore, *Altabet* [1988] did not measure DON, which could account for a substantial amount of the nitrogen export [*Carlson et al.*, 1994]. One is thus led to conclude that although $\delta^{15}N$ measurements show great potential, the measurements available to date are insufficient to support or disprove the nitrogen fixation hypothesis that we propose (M. A. Altabet, personal communication, 1996).

What is the reason for the existence of a large positive N^* signal due to nitrogen fixation in the North Atlantic and for the absence of a similar N^* signal in the other basins? Because of nitrogen limitation, the oligotrophic waters in the other regions would equally favor N_2 fixation as is observed in the North Atlantic. Part of the explanation is related to the fact that N^* reflects the combined effect of N_2 fixation and denitrification. In the Indian Ocean the influence of denitrification is overwhelming most of the signal that is generated by N_2 fixation. However, this is much less the case in the Pacific Ocean and in the South Atlantic.

It has been suggested that iron may play a crucial role in limiting the growth of diazotrophic organisms [*Rueter et al.*, 1992] and that therefore the observed spatial patterns of N_2 fixation may be coupled with the availability of this micronutrient [*Galloway et al.*, 1995; *Michaels et al.*, 1996]. The diazotrophic metabolism that allows species like *Trichodesmium* to grow in nitrogen-poor oligotrophic oceans relies on many iron-containing enzymes and proteins, leading to a nitrogen-to-iron ratio that is 1 to 2 orders of magnitude greater than that of other oceanic organisms [*Geider and La Roche*, 1994]. The high iron requirement of these organisms is problematic in light of the often limited delivery of iron to the open ocean. *Duce et al.* [1991] estimated the atmospheric mineral dust input to the world oceans and found order of magnitude differences between ocean regions. In general, fluxes of mineral dust to the ocean basins are a factor of about 10 higher in the northern hemisphere than in the southern hemisphere, with the North Pacific obtaining about the same amount of mineral dust as the North Atlantic. Assuming that the average iron content of dust (about 3.5%) does not vary greatly [*Donaghay et al.*, 1991], the distribution of dust supply is directly related to the iron supply. This argument may explain the large difference in N^* between the North Atlantic and the South Atlantic but fails for the North Pacific Ocean. However, closer inspection of the spatial distribution of dust deposition in the North Atlantic and North Pacific [*Duce et al.*, 1991] reveals that the dust flux in the North Pacific is largely confined to the western Pacific, whereas the North Atlantic receives large amounts of dust across the entire basin. Furthermore, differences in the temporal supply of dust may significantly affect how the supplied

iron can be used by the marine organisms [*Donaghay et al.*, 1991]. *Michaels et al.* [1996] calculated that the iron requirement by diazotrophs at station BATS is comparable to the rates supplied by deposition of iron from Saharan dust. Interannual variability in iron inputs are large at this site and could cause comparable variations in the nitrogen fixation rate [*Michaels et al.*, 1996]. Observations of dust concentrations at Barbados indicate a threefold increase between the period before 1970 and thereafter, probably associated with the expansion of the Sahara [*Michaels et al.*, 1996]. If dust supply controls the amount of N_2 fixation, we expect that such increases in dust concentrations should lead to equal increases of N_2 fixation.

To check this possibility, we compare N^* data in the northwestern Sargasso Sea from GEOSECS (1972/1973), TTO NAS (1981), and the U.S. JGOFS time series station BATS (1988-1995) [*Knap et al.*, 1991, 1992, 1993, 1994]. We reduce P data from BATS after March 1991 by 0.05 μmol kg^{-1} in order to bring the deep ocean values (<2000 m) in agreement with the first 3 years at BATS and data from GEOSECS and TTO. This correction is necessary because of the systematic changes that occurred as a consequence of a change in the measurement method [*Michaels and Knap*, 1996; A. F. Michaels, personal communication, 1996]. We find statistically significant changes at the 5% significance level tested with a student t test in the depth range of the vertical N^* maximum from 200 to 700 m with N^* being on average about 0.5 μmol kg^{-1} higher during BATS (1988-1995) compared to TTO and GEOSECS 1 or 2 decades earlier. The thermocline ventilates on a timescale of years to decades, so the N^* signal is a low-pass-filtered signal of the N_2 fixation history over approximately a decade before the observation. The increase in N^* that we see in the thermocline would therefore be consistent with the observed increase of iron deposition over Barbados. This conclusion remains, however, speculative because the observed increase depends almost entirely on the 0.05 μmol kg^{-1} correction applied to the BATS P data. Furthermore, the stations selected for GEOSECS and TTO are on average more than 500 km away from the BATS location, and therefore a part of the observed change might be due to horizontal rather than temporal variability. We therefore cannot give a definitive answer whether or not N^* increased over the last 2 decades in the subtropical North Atlantic consistent with the hypothesis that the atmospheric deposition of iron is a controlling factor for N_2 fixation.

Global Marine Nitrogen Budget and Implications for the Carbon Cycle

We now discuss the implications of our North Atlantic nitrogen fixation estimate for the global marine nitrogen budget. Our N_2 fixation estimate is about 22 times that of *Capone and Carpenter* [1982] in the same region (Table 3). Their estimate does not, however, take the contribution of blooms into account. On a global basis, inclusion of the contribution of blooms doubles their total pelagic N_2 fixation estimate [*Carpenter and Capone*, 1992] (Table 3). Assuming that the same ratio applies for the North Atlantic, we doubled their total pelagic N_2 fixation in the North Atlantic to about 2.6 Tg N yr^{-1}, which is about 11 times smaller than our estimate. If this ratio is carried over to the other oceans, then the global pelagic nitrogen fixation rate would have to be increased from 10 Tg N yr^{-1} to about 110 Tg N yr^{-1}. A similar value would be found if one assumed that N_2 fixation is only taking place in the tropical and subtropical oceans from 30°S to 30°N and that the areal fixation rate in the Indian Ocean is the same as in the Atlantic and that in the Pacific this rate is only a quarter of the Atlantic rate. We assign a large error of about 40 Tg N yr^{-1} to our tentative extrapolation. If we put this number into an updated version of the global marine nitrogen cycle based on a literature survey, we find a more or less balanced budget for both preindustrial and current times (see Table 4). This updated version does not include, however, the upwardly revised estimates of benthic denitrification that L. A. Codispoti et al. (personal communication, 1995) have proposed.

Such a more or less balanced budget differs from the budgets of *Codispoti and Christensen* [1985] (see Table 4) and *Codispoti* [1989], who propose that the present marine N budget could have a deficit of the order of 70 Tg N yr^{-1}. However, our uncertainties also encompass the possibility of a marine nitrogen budget with imbalances of this magnitude. We are thus presently not able to draw a final conclusion whether the marine nitrogen budget is closed or not. Nevertheless, it is of interest to ask what would be the consequences for the marine carbon cycle and atmospheric CO_2 if we assume that the ocean is indeed losing nitrogen with an annual rate of 70 Tg N yr^{-1}? Assuming that global new production is limited mainly by nitrogen and and that new production has a C:N stoichiometry of 117:16, a removal of 70 Tg N yr^{-1} results in a yearly decrease of oceanic new production of about 0.4 GT C yr^{-1}. We estimate that such a decrease leads to a negative net air-sea transfer of CO_2 of the order of 0.07 GT C yr^{-1} based on the results of the ocean general circulation model (OGCM) simulations of *Orr and Sarmiento* [1992]. Such a net air-sea exchange flux is not permitted to be operative for periods longer than about 300 years, in order to keep atmospheric CO_2 concentrations within the observed variability of 280 ± 10 ppm during the last millennium before the onset of the anthropogenic perturbation [*Barnola et al.*, 1995]. If the present-day net loss of 70 Tg N yr^{-1} is real, then the ocean must have been in a state of stationary oscillations between net

Table 4. Estimated Sources and Sinks in the Global Marine Nitrogen Budget Based on *Codispoti and Christensen* [1985], This Study, and a Survey of the Recent Literature

Process	Modified From *Codispoti and Christensen* [1985],	This Study and Literature Survey	
	Preindustrial, Tg N yr^{-1}	Preindustrial, Tg N yr^{-1}	Current, Tg N yr^{-1}
	Sources		
Pelagic N_2 fixation	25	110 ± 40[a]	110 ± 40[a]
Benthic N_2 fixation		15 ± 10[b]	15 ± 10[b]
River input (DON)	25	20 ± 10[c]	34 ± 10[c]
River input (PON)		21 ± 10[c]	42 ± 10[c]
Atmospheric deposition	24[d]	15 ± 5[e]	30 ± 5[e]
Total sources	74	181 ± 44	231 ± 44
	Sinks		
Benthic denitrification	60	85 ± 20[f]	95 ± 20[f]
Water column denitrification	60	80 ± 20[g]	80 ± 20[g]
Sedimentation	21	15 ± 5[h]	25 ± 10[h]
N_2O loss	1	4 ± 2[i]	4 ± 2[i]
Total sinks	142	184 ± 29	204 ± 30

Uncertainty estimates based on ranges given in the literature. DON, dissolved organic nitrogen; PON, particulate organic nitrogen.

[a]Extrapolation from our estimate of the tropical and Subtropical North Atlantic (see text).

[b]Based on *Capone* [1983].

[c]Based on *Meybeck* [1982], *Duce et al.* [1991], and *Galloway et al.* [1995].

[d]Reduced from the value given by *Codispoti and Christensen* [1985] to account for the organic N loss from the ocean to the atmosphere.

[e]Based on *Duce et al.* [1991] and *Galloway et al.* [1995].

[f]Based on *Codispoti and Christensen* [1985], *Galloway et al.* [1995], and the assumption that half of the anthropogenic PON river flux is denitrified.

[g]Based on *Christensen et al.* [1987].

[h]Based on *Wollast* [1991] and the assumption that half of the anthropogenic PON river flux is sedimented.

[i]Based on *Prather et al.* [1994] and P. Suntharalingam (personal communication, 1996).

gain of nitrogen and net loss over the latest part of the Holocene with a timescale of about 300 years. This is much shorter than the proposed feedback mechanism of *Codispoti* [1989], which involves changes in new production that causes subsurface oxygen concentrations to change, thereby changing denitrification. *Codispoti* [1989] estimates that this feedback has a timescale of about 1000 years.

The deficit in the nitrogen budgets of *Codispoti and Christensen* [1985] and *Codispoti* [1989] has been taken as support for the hypothesis of *McElroy* [1983], who proposed that the ocean oscillates between a state of excess fixed nitrogen during glacial periods and a state of deficit during interglacial periods. Our nitrogen budget does not support such a large deficit in nitrogen sources, but the uncertainties are too great to be able to say anything definitive about this issue.

Summary and Conclusions

We define a new quasi-conservative tracer N^* based on the assumptions of constant stoichiometric ratios during (1) nitrification of organic matter, (2) denitrification of nitrate coupled with the mineralization of organic matter, and (3) production of nitrogen-rich organic matter by nitrogen fixing organisms (diazotrophs). The variability of this new tracer reflects only the source minus sinks terms due to the processes of denitrification and N_2 fixation. We calculate N^* using GEOSECS data for the global distribution and data from eight other field programs for the Atlantic Ocean.

The global distribution of N^* is characterized by high values in the North Atlantic Ocean and in the Mediterranean, intermediate concentrations in the Southern Ocean and over large parts of the North and tropical

Pacific, and low concentrations in the Indian Ocean and in the eastern Pacific. The observed pattern coincides well with direct studies of denitrification and N_2 fixation. This in turn supports our a priori assumption of a near-constant stoichiometric ratio during nitrification of organic matter because N^*, which represents deviations from this stoichiometric ratio, shows a very consistent spatial pattern in accordance with the known distribution of denitrification and N_2 fixation. Our findings are also consistent with the results of *Anderson and Sarmiento* [1994], who suggested that the nitrate deficit they observed in the intermediate waters of the Atlantic, Pacific, and Indian Oceans is caused by denitrification.

Our analysis suggests that on a global scale the North Atlantic Ocean and the Mediterranean are major sources of fixed nitrogen, whereas the Indian Ocean and parts of the Pacific Ocean are sinks. The sink regions of the ocean are associated with the major regions of anoxia in the thermocline of the Arabian Sea and in the northern and southern equatorial Pacific where denitrification is well known to occur. Sedimentary denitrification in the Bering Sea, in the eastern Pacific shelf regions, and to a lesser extent in the shelf regions of eastern North America also acts as sinks for N^*. More detailed analysis of the source region in the North Atlantic reveals that it is confined to the tropical and subtropical North Atlantic.

We estimate nitrogen fixation in the North Atlantic in the region from 10°N to 50°N by using N^* observations on isopycnal surfaces together with concurrent helium-3 and tritium observations. We find a nitrogen fixation rate of 20×10^{11} mol N yr^{-1} or 28 Tg N yr^{-1}. This is an order of magnitude larger than previous estimates for the same region but in accordance with more recent studies suggesting that N_2 fixation has been severely underestimated. We show that the nitrogen contribution by N_2 fixation is sufficient to meet the estimated N demand by the mixed layer ecosystem at the U.S. JGOFS BATS time series station, which is otherwise difficult to explain by atmospheric N deposition or vertical transport from below. Measurements of $\delta^{15}N$ of organic matter would offer the potential to test our hypothesis that N_2 fixation contributes significantly to the nitrogen cycle in this region, but the measurements available to date are insufficient to do so.

The reasons why N_2 fixation seems to be high in the North Atlantic and less important in the Pacific are less clear. It has been suggested that spatial and temporal differences in the atmospheric supply of iron, which is needed in large quantities by organisms capable of N_2 fixation, may play an essential role in determining the spatial distribution of N_2 fixation [*Galloway et al.*, 1995; *Michaels et al.*, 1996].

A tentative extrapolation of our calculated N_2 fixation rate in the Atlantic Ocean to the world oceans, and a summary of literature values for the other processes, permits us to present a more or less balanced budget for both the preindustrial and present marine nitrogen cycle. We believe that other budgets which propose current imbalances of the order of 100 Tg N yr^{-1} are unlikely. However, the uncertainties in the marine nitrogen budget are still too large to draw a final conclusion. In any case, there is increasing evidence that the marine N cycle is much more dynamic than had been thought 10 years ago [*Codispoti*, 1995].

At present we lack nutrient data with a resolution high enough to investigate the distribution of N^* in more detail on a global scale. We also lack concurrent transient tracer data to calculate the rates of denitrification and N_2 fixation in regions other than the tropical and subtropical North Atlantic. The data from the ongoing World Ocean Circulation Experiment (WOCE) will soon provide the opportunity to analyze the distribution of N^* in more detail, and N^*-based estimates of denitrification and N_2 fixation might then help to narrow the large uncertainties that are presently associated with the marine nitrogen cycle.

Appendix: Data Considerations

Measurement Methods, Precision, and Accuracy

The nutrient data during the GEOSECS program have been measured using standard colorimetric methods. The deep water sampling precision during these cruises was evaluated by the determination of replicate samples and calculation of the standard deviation of samples taken from a deep water adiabatic water column [*Bainbridge*, 1981; *Broecker et al.*, 1982; *Weiss et al.*, 1983]. These studies reported relative standard deviations of 0.0–0.8% for nitrate and 0–1.4% for phosphate. Taking the global average deep water concentration of 32 μmol kg^{-1} for nitrate and 2.2 μmol kg^{-1} for phosphate, we estimate conservatively the precision of the GEOSECS nutrient analysis to be 0.26 μmol kg^{-1} for nitrate and 0.03 μmol kg^{-1} for phosphate.

The TTO (1981-1983), Oceanus 133-7 (1983), Atlantis 109 (1981), SAVE (1987-1989), Oceanus 202 (1988), AJAX (1983-1984) and *Meteor* 11/5 (1991) cruises provide high-quality nutrient data obtained by the use of standard automated colorimetric methods. The overall sampling and analysis precision of the nutrient analysis during these cruises is estimated to be 0.1 μmol kg^{-1} for nitrate and 0.01 μmol kg^{-1} for phosphate based on replicate samples.

Internal Consistency

We investigated the internal consistency of the Atlantic data sets by determining deep ocean (>3500 m) N, P, and salinity trends versus potential temperature at (1) reoccupied or closely revisited stations and in (2) 10° by 10° areas that have been repeatedly sampled by the different cruises. Both methods gave very similar

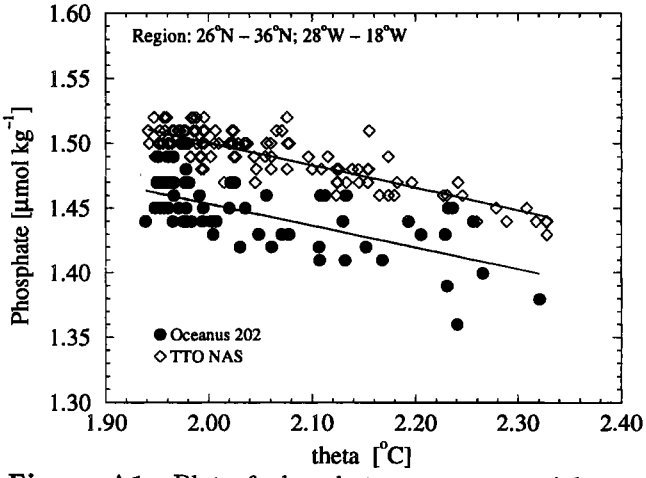

Figure A1. Plot of phosphate versus potential temperature (theta) in the region from 26°N to 36°N and from 28°W to 18°W and for depths below 3500 m. Data from Oceanus 202 are shown by solid circles, and data from TTO NAS are shown by open diamonds. The solid lines represent the results of linear regressions. A mean difference of 0.065 μmol kg^{-1} has been found between the two cruises.

results, and we report here only the results from the second method. Nutrient data from GEOSECS, TTO, SAVE, Atlantis 109, and AJAX revealed no systematic differences. However, systematic offsets were identified for Oceanus 202, Oceanus 133-7, and *Meteor* 11/5.

Comparison of P versus potential temperature in the region from 26°N to 36°N and from 28°W to 18°W and below 3500 m show a significant systematic difference between Oceanus 202 and the TTO NAS cruise of approximately –0.07 μmol kg^{-1} (Figure A1). Very

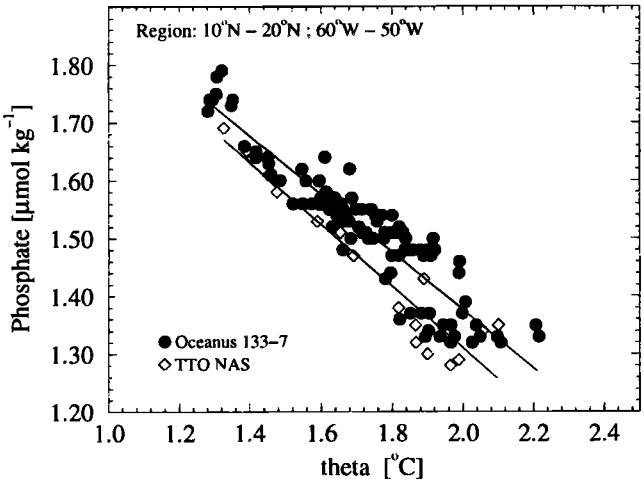

Figure A2. Plot of phosphate versus potential temperature (theta) in the region from 10°N to 20°N and from 60°W to 50°W and for depths below 3500 m. Data from Oceanus 133-7 are shown by solid circles, and data from TTO NAS are shown by open diamonds. The solid lines represent the results of linear regressions. A mean difference of 0.060 μmol kg^{-1} has been found between the two cruises.

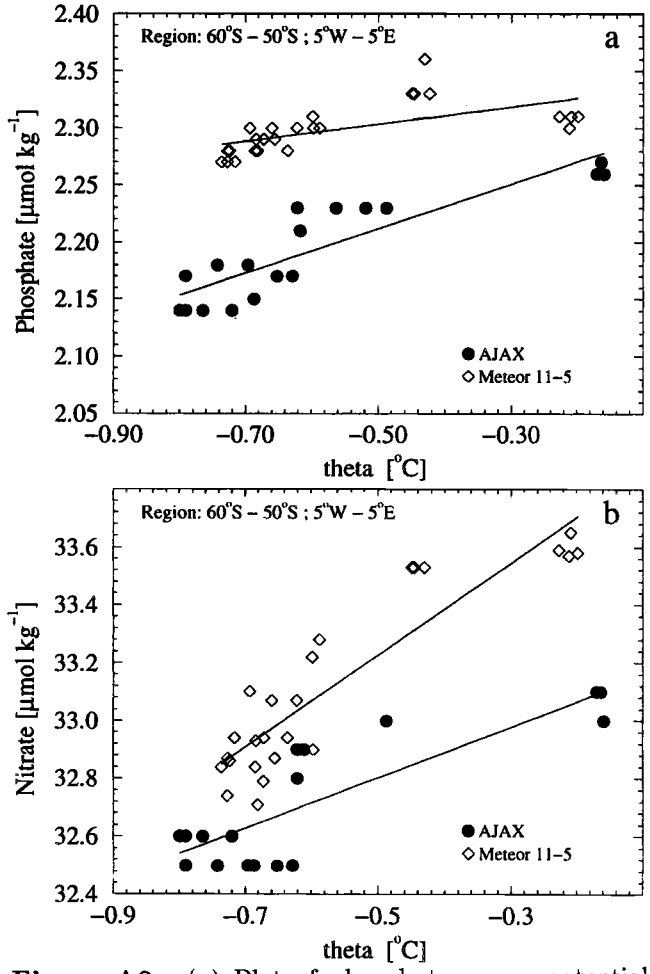

Figure A3. (a) Plot of phosphate versus potential temperature (theta) in the region from 60°S to 50°S and from 5°W to 5°E and for depths below 3500 m. Data from AJAX are shown by solid circles, and data from *Meteor* 11/5 are shwon by open diamonds. The solid lines represent the results of linear regressions. A mean difference of 0.074 μmol kg^{-1} has been found for phosphate between the two cruises. (b) Plot of nitrate versus potential temperature (theta) in the same region and also for depths below 3500 m. For nitrate a mean difference of 0.44 μmol kg^{-1} has been calculated.

similar offsets were found in comparison with Atlantis 109, TTO TAS, SAVE, and GEOSECS in six other 10° by 10° regions (mean difference of –0.055 ± 0.019 μmol kg^{-1}). No significant offsets could be identified for salinity (–0.002 ± 0.002 psu) and nitrate (–0.10 ± 0.13 μmol kg^{-1}), and we therefore conclude that this offset in P is due to analytical problems and should be corrected for.

Oceanus 133-7 also revealed a systematic offset in the P determination. Figure A2 shows P versus potential temperature in the region from 10°N to 20°N and from 60°W to 50°W and below 3500 m for data from the Oceanus 133-7 and TTO NAS cruises. P data from Oceanus 133-7 appear to be about 0.06 μmol kg^{-1} higher

than the data from TTO NAS. Identical plots for salinity and nitrate show no such offsets. Comparison of Oceanus 133-7 versus GEOSECS and TTO TAS in the same region gave the similar results (mean differences of 0.001 ± 0.002 psu for salinity, -0.03 ± 0.13 μmol kg^{-1} for N, and 0.055 ± 0.005 μmol kg^{-1} for P) supporting our view that the offset in P is quite probably not "real".

The consistency of the nutrient data of the *Meteor* 11/5 cruise with the nutrient data from the AJAX cruise is shown in Figure A3, where P and N are plotted versus potential temperature in the region from 60°S to 50°S and from 5°W to 5°E, respectively. We calculated a systematic offset between these two cruises of approximately 0.5 μmol kg^{-1} for N and of 0.07 μmol kg^{-1} for P. Comparison of these two cruises in five more 10° by 10° regions yielded similar findings for the nutrients (0.5 ± 0.3 μmol kg^{-1} for N and 0.05 ± 0.03 μmol kg^{-1} for P) but did not show significant differences for salinity (-0.002 ± 0.002 psu). Comparison of *Meteor* 11/5 with nutrient data from GEOSECS in five regions showed higher differences (1.0 ± 0.2 μmol kg^{-1} for N and 0.07 ± 0.03 μmol kg^{-1} for P) consistent with a existing but only hardly significant difference between AJAX and GEOSECS (0.003 ± 0.002 psu for salinity, 0.4 ± 0.3 μmol kg^{-1} for N, and 0.03 ± 0.03 μmol kg^{-1} for P). We decided to correct the *Meteor* 11/5 data only by the difference found in comparison to the more modern AJAX data.

In summary, we applied the following corrections to the Atlantic nutrient data sets:

Oceanus 202	: $P_{corr} = P_{meas} + 0.05$ μmol kg^{-1}
Oceanus 133-7	: $P_{corr} = P_{meas} - 0.05$ μmol kg^{-1}
Meteor 11/5	: $P_{corr} = P_{meas} - 0.05$ μmol kg^{-1}
Meteor 11/5	: $N_{corr} = N_{meas} - 0.5$ μmol kg^{-1}

Acknowledgments. The first thanks go to all the scientists and personnel on the research ships that collected the high-quality nutrient data that made this study possible. Most of the ideas presented in this paper have been developed during the 1-year sabbatical visit of J.L.S. with the Division of Climate and Environmental Physics of the Physics Institute. We are indebted to T.F. Stocker for making this visit possible and for his continuing support to the first author. We are grateful to R. Key for helping us in data acquisition and providing us the Le Traon code for objective analysis. W.J. Jenkins is due thanks for making his tritium and helium isotope data in the North Atlantic available to us. We thank F. Joos and O. Marchal for valuable discussions during the preparation of this article. Reviews by A.F. Michaels and L.A. Codispoti helped to improve the article. We appreciate the efforts of M. Bender who served as editor for this article. N.G. was supported by the Swiss National Science Foundation. J.L.S. was granted support by the National Science Foundation (OCE-9314707 and OCE-9402633).

References

Altabet, M. A., Variations in nitrogen isotopic composition between sinking and suspended particles: Implications for nitrogen cycling and particle transformation in the open ocean, *Deep Sea Res., Part A, 35*, 535–554, 1988.

Altabet, M. A., and J. J. McCarthy, Temporal and spatial variations in the natural abundance of ^{15}N in PON from a warm-core ring, *Deep Sea Res., Part A, 32*, 755–772, 1985.

Anderson, J. J., A. Okubo, A. S. Robbins, and F. A. Richards, A model for nitrite and nitrate distributions in oceanic oxygen minimum zones, *Deep Sea Res., Part A, 29*, 1113–1140, 1982.

Anderson, L. A., On the hydrogen and oxygen content of marine phytoplankton, *Deep Sea Res., Part I, 42*, 1675–1680, 1995.

Anderson, L. A., and J. L. Sarmiento, Redfield ratios of remineralization determined by nutrient data analysis, *Global Biogeochem. Cycles, 8*, 65–80, 1994.

Bainbridge, A., *Hydrographic Data, 1972-1973, GEOSECS Atlantic Expedition*, vol. 1, U.S. Govt. Print. Off., Washington, D. C., 1981.

Barnes, R. O., K. K. Bertine, and E. D. Goldberg, N_2:Ar, nitrification and denitrification in southern California borderland basin sediments, *Limnol. Oceanogr., 20*, 963–970, 1975.

Barnola, J. M., M. Anklin, J. Porcheron, D. Raynaud, J. Schwander, and B. Stauffer, CO_2 evolution during the last millennium as recorded by Antarctic and Greenland ice, *Tellus, Ser. B., 47*, 264–272, 1995.

Béthoux, J., and G. Copin-Montégut, Biological fixation of atmospheric nitrogen in the Mediterranean Sea, *Limnol. Oceanogr., 31*, 1353–1358, 1986.

Béthoux, J., P. Morin, C. Madec, and B. Gentili, Phosphorus and nitrogen behaviour in the Mediterranean Sea, *Limnol. Oceanogr., 39*, 1641–1654, 1992.

Boulahdid, M., and J. F. Minster, Oxygen consumption and nutrient regeneration ratios along isopycnal horizons in the Pacific Ocean, *Mar. Chem., 26*, 133–153, 1989.

Brandhorst, W., Nitrification and denitrification in the eastern tropical North Pacific, *J. Cons. Int. Explor. Mer., 25*, 3–20, 1959.

Brewer, P. G., W. S. Broecker, W. J. Jenkins, P. B. Rhines, C. G. Rooth, J. H. Swift, T. Takahashi, and R. T. Williams, A climate freshening of the deep Atlantic north of 50°N over the past 20 years, *Science, 222*, 1237–1239, 1983.

Broecker, W. S., 'NO', a conservative water-mass tracer, *Earth Planet. Sci. Lett., 23*, 100–107, 1974.

Broecker, W. S., Chemical signatures associated with the freshening of Northern Atlantic waters between 1972 and 1982, North Atlantic Deep Water Formation, *NASA Conf. Publ., 2367*, 13–17, 1985.

Broecker, W. S., and T.-H. Peng, *Tracers in the Sea*, Eldigio, Lamont-Doherty Geol. Obs., Palisades, N.Y., 1982.

Broecker, W. S., D. Spencer, and H. Craig, *Hydrographic Data, 1973-1974, GEOSECS Pacific Expedition*, vol. 3, U.S. Govt. Print. Off., Washington, D. C., 1982.

Broecker, W. S., T. Takahashi, and T. Takahashi, Sources and flow patterns of deep-ocean waters as deduced from potential temperature, salinity, and initial phosphate concentration, *J. Geophys. Res., 90*, 6925–6939, 1985.

Broecker, W. S., S. Blanton, W. M. Smethie, and G. Ostlund, Radiocarbon decay and oxygen utilization in the deep Atlantic Ocean, *Global Biogeochem. Cycles, 5*, 87–117, 1991.

Bryden, H., New polynomials for thermal expension, adiabatic temperature gradient and potential temperature of sea water, *Deep Sea Res., 20*, 401–408, 1973.

Buesseler, K. O., A. F. Michaels, D. A. Siegel, and A. H. Knap, A three-dimensional time-dependent approach to calibrating sediment trap fluxes, *Global Biogeochem. Cycles, 8*, 179–193, 1994.

Burkill, P. H., R. F. C. Mantoura, and N. J. P. Owens, Biogeochemical cycling in the northwestern Indian Ocean: A brief overview, *Deep Sea Res., Part II, 40*, 643–649, 1993.

Capone, D., A. Subramaniam, E. Carpenter, J. Montoya, and C. Humborg, A spatially and temporally extensive bloom of the diazotrophic cyanobacterium *Trichodesmium* in the central Arabian Sea during the spring intermonsoon, *EOS, Trans. AGU, 76*, OS2, 1996.

Capone, D. G., Benthic nitrogen fixation, in *Nitrogen in the Marine Environment*, edited by E. J. Carpenter and D. G. Capone, pp. 105–137, Academic, San Diego, Calif., 1983.

Capone, D. G., and E. J. Carpenter, Nitrogen fixation in the marine environment, *Science, 217*, 1140–1142, 1982.

Carlson, C. A., H. W. Ducklow, and A. F. Michaels, Annual flux of dissolved organic carbon from the euphotic zone in the northwestern Sargasso Sea, *Nature, 371*, 405–408, 1994.

Carpenter, E., and C. Price, Nitrogen fixation, distribution, and production of *Oscillatoria* (*Trichodesmium*) spp. in the western Sargasso and Caribbean Seas, *Limnol. Oceanogr., 22*, 60–72, 1977.

Carpenter, E. J., Nitrogen fixation by marine Oscillatoria (*Trichodesmium*) in the world's oceans, in *Nitrogen in the Marine Environment*, edited by E. J. Carpenter and D. G. Capone, pp. 65–103, Academic, San Diego, Calif., 1983.

Carpenter, E. J., and D. G. Capone, Nitrogen fixation in Trichodesmium blooms, in *Marine Pelagic Cyanobacteria: Trichodesmium and other Diazotrophs*, edited by E. J. Carpenter, pp. 211–217, Kluwer Acad., Norwell, Mass., 1992.

Carpenter, E. J., and K. Romans, Major role of the cyanobacterium *Trichodesmium* in nutrient cycling in the North Atlantic Ocean, *Science, 254*, 1356–1358, 1991.

Carpenter, E. J., M. I. Scranton, P. C. Novelli, and A. F. Michaels, Validity of N_2 fixation rate measurements in marine Oscillatoria (*Trichodesmium*), *J. Plankton Res., 9*, 1047–1056, 1987.

Chipman, D., T. Takahashi, D. Breger, and S. Sutherland, Carbon dioxide, hydrographic, and chemical data obtained during the R/V *Meteor* cruise 11/5 in the South Atlantic and Northern Weddell Sea areas (WOCE sections A-12 and A-21), *Data Rep., ORNL/CDIAC-55; NDP-045*, Carbon Dioxide Inf. Anal. Cent., Oak Ridge Natl. Lab., Oak Ridge, Tenn., 1994.

Christensen, J. P., J. W. Murray, A. H. Devol, and L. A. Codispoti, Denitrification in continental shelf sediments has major impact on the oceanic nitrogen budget, *Global Biogeochem. Cycles, 1*, 97–116, 1987a.

Christensen, J. P., J. W. Smethie, and A. H. Devol, Benthic nutrient regeneration and denitrification on the Washington continental shelf, *Deep Sea Res., 34*, 1027–1047, 1987b.

Cline, J. D., and I. R. Kaplan, Isotopic fractionation of dissolved nitrate during denitrification in the eastern tropical North Pacific Ocean, *Mar. Chem., 3*, 271–299, 1975.

Cline, J. D., and F. A. Richards, Oxygen deficient conditions and nitrate reduction in the eastern tropical North Pacific ocean. *Limnol. Oceanogr., 17*, 885–900, 1972.

Codispoti, L. A., Phosphorus vs. nitrogen limitation of new and export production, in *Productivity of the Ocean: Present and Past*, edited by W. H. Berger, V. S. Smetacek, and G. Wefer, pp. 377–394, John Wiley, New York, 1989.

Codispoti, L. A., Is the ocean losing nitrate ?, *Nature, 376*, 724, 1995.

Codispoti, L. A., and J. P. Christensen, Nitrification, denitrification and nitrous oxide cycling in the eastern tropical South Pacific Ocean, *Mar. Chem., 16*, 277–300, 1985.

Codispoti, L. A., and T. T. Packard, Denitrification rates in the eastern tropical South Pacific, *J. Mar. Res., 38*, 453–477, 1980.

Codispoti, L. A., and F. A. Richards, An analysis of the horizontal regime of denitrification in the eastern tropical North Pacific, *Limnol. Oceanogr., 21*, 379–388, 1976.

Codispoti, L. A., G. E. Friederich, and D. W. Hood, Variability in the inorganic carbon system over the southeastern Bering Sea shelf during spring 1980 and spring-summer 1981, *Cont. Shelf Res., 5*, 133–160, 1986.

Coles, V. J., M. S. McCartney, D. B. Olson, and W. M. Smethie, Changes in Antarctic Bottom Water properties in the western South Atlantic in the late 1980s, *J. Geophys. Res., 101*, 8957–8970, 1996.

Conkright, M., S. Levitus, and T. Boyer, NOAA Atlas NESDIS 1: World ocean atlas 1994, vol. 1, Nutrients, technical report, Natl. Oceanic and Atmos. Admin., Silver Spring, Md., 1994.

Deuser, W. G., E. H. Ross, and Z. J. Mlodzinska, Evidence for and rate of denitrification in the Arabian Sea, *Deep Sea Res., 25*, 431–445, 1978.

Devol, A. H., Direct measurements of nitrogen gas fluxes from continental shelf sediments, *Nature, 349*, 319–321, 1991.

Donaghay, P. L., P. S. Liss, R. A. Duce, D. R. Kester, A. K. Hanson, R. Villareal, N. W. Tindale, and D. J. Gifford, The role of episodic atmospheric nutrient inputs in the chemical and biological dynamics of oceanic ecosystems, *Oceanography, 4*, 62–70, 1991.

Duce, R., The impact of atmospheric nitrogen, phosphorus and iron species on marine biological productivity., in *The Role of Air-Sea Exchange in Geochemical Cycling*, edited by P. Buat-Ménard, pp. 497–529, D. Reidel, Norwell, Mass., 1986.

Duce, R. A., et al., The atmospheric input of trace species to the world ocean, *Global Biogeochem. Cycles, 5*, 193–259, 1991.

Fanning, K. A., Influence of atmospheric pollution on nutrient limitation in the ocean, *Nature, 339*, 460–463, 1989.

Fanning, K. A., Nutrient provinces in the sea: Concentration ratios, reaction rate ratios, and ideal covariation, *J. Geophys. Res., 97*, 5693–5712, 1992.

Fiadeiro, M., and J. D. H. Strickland, Nitrate reduction and the occurrence of a deep nitrite maximum in the ocean off the West Coast of South America, *J. Mar. Res., 26*, 187–201, 1968.

Fofonoff, N., Computation of potential temperature of seawater for an arbitrary reference pressure, *Deep Sea Res., 24*, 489–491, 1977.

Galloway, J. N., W. H. Schlesinger, H. Levy II, A. Michaels, and J. L. Schnoor, Nitrogen fixation: Anthropogenic enhancement-environmental response, *Global Biogeochem. Cycles, 9*, 235–252, 1995.

Ganeshram, R. S., T. F. Pedersen, S. E. Calvert, and J. W. Murray, Large changes in oceanic nutrient inventories from glacial to interglacial periods, *Nature, 376*, 755–758, 1995.

Geider, R. J., and J. La Roche, The role of iron in phytoplankton photosynthesis and the potential for iron-limitation of primary productivity in the sea, *Photosynth. Res., 39*, 275–301, 1994.

Goering, J., R. Dugdale, and D. Menzel, Estimates of in situ rates of nitrogen uptake by *Trichodesmium spp* in the tropical Atlantic Ocean, *Limnol. Oceanogr., 11*, 614–620, 1966.

Goering, J., F. Richards, L. Codispoti, and R. Dugdale,

Nitrogen fixation and denitrification in the ocean : Biogeochemical budgets, in *Hydrogeochemistry and Biogeochemistry*, edited by E. Ingerson, pp. 12–27, Clarke, Ontario, Canada, 1973.

Haines, J., R. Atlas, R. Griffiths, and R. Morita, Denitrification and nitrogen fixation in Alaskan continental shelf sediments, *Appl. Environ. Microbiol., 41*, 412–421, 1981.

Hattori, A., Denitrification and dissimilatory nitrate reduction, in *Nitrogen in the Marine Environment*, edited by E. J. Carpenter and D. G. Capone, pp. 191–232, Academic, San Diego, Calif., 1983.

Hoering, T. C., and H. T. Ford, The isotope effect in the fixation of nitrogen by *Azotobacter*, *J. Am. Chem. Soc., 82*, 376–378, 1960.

Jenkins, W. J., Tritium and ^{3}He in the Sargasso sea, *J. Mar. Res., 38*, 533–569, 1980.

Jenkins, W. J., ^{3}H and ^{3}He in the Beta Triangle: Observations of gyre ventilation and oxygen utilization rates, *J. Phys. Oceanogr., 17*, 763–783, 1987.

Jenkins, W. J., and D. W. R. Wallace, Tracer based inferences of new primary production in the sea, in *Primary Productivity and Biogeochemical Cycles in the Sea*, edited by P. G. Falkowski and A. D. Woodhead, pp. 299–316, Plenum, New York, 1992.

Johnson, D. L., and M. E. Q. Pilson, Spectrophotometric determination of arsenite, arsenate, and phosphate in natural waters, *Anal. Chim. Acta, 58*, 289–299, 1972.

Karl, D. M., R. Letelier, D. V. Hebel, D. F. Bird, and C. D. Winn, Trichodesmium blooms and new production in the North Pacific gyre, in *Marine Pelagic Cyanobacteria: Trichodesmium and other Diazotrophs*, edited by E. J. Carpenter, pp. 219–237, Kluwer Acad., Norwell, Mass., 1992.

Kawase, M., and J. L. Sarmiento, Nutrients in the Atlantic thermocline, *J. Geophys. Res., 90*, 8961–8979, 1985.

Knap, A. H., et al., Data report for BATS 1–BATS 12, October, 1988–September 1989, Bermuda Bio. Sta. Res., Inc., U.S. Joint Global Ocean Flux Study, *Tech. Rep. BATS Data Rep. B-1*, U.S. Joint Global Ocean Flux Study Planning Office, Woods Hole, Mass., 1991.

Knap, A. H., et al., Data report for BATS 13–BATS 24, October, 1989–September 1990, Bermuda Bio. Sta. Res., Inc., U.S. Joint Global Ocean Flux Study, *Tech. Rep. BATS Data Rep. B-2*, U.S. Joint Global Ocean Flux Study Planning Office, Woods Hole, Mass., 1992.

Knap, A. H., et al., Data report for BATS 25–BATS 36, October, 1990–September 1991, Bermuda Bio. Sta. Res., Inc., U.S. Joint Global Ocean Flux Study, *Tech. Rep. BATS Data Rep. B-3*, U.S. Joint Global Ocean Flux Study Planning Office, Woods Hole, Mass., 1993.

Knap, A. H., et al., Data report for BATS 37–BATS 48, October, 1991–September 1992, Bermuda Bio. Sta. Res., Inc., U.S. Joint Global Ocean Flux Study, *Tech. Rep. BATS Data Rep. B-4*, U.S. Joint Global Ocean Flux Study Planning Office, Woods Hole, Mass., 1994.

Koike, I., and A. Hattori, Estimates of denitrification in sediments of the Bering Sea shelf, *Deep Sea Res., Part A, 26*, 409–415, 1979.

LeTraon, P. Y., A method for optimal analysis of fields with spatially variable mean, *J. Geophys. Res., 95*, 13543–13547, 1990.

Levitus, S., and T. Boyer, NOAA Atlas NESDIS 2: World ocean atlas 1994, vol. 2, Oxygen, technical report, Natl. Oceanic and Atmos. Admin., Silver Spring, Md., 1994a.

Levitus, S., and T. Boyer, NOAA Atlas NESDIS 4: World ocean atlas 1994, vol. 4, Temperature, technical report, Natl. Oceanic and Atmos. Admin., Silver Spring, Md., 1994b.

Levitus, S., R. Burgett, and T. Boyer, NOAA Atlas NESDIS 3: World ocean atlas 1994, vol. 3, Salinity, technical report, Natl. Oceanic and Atmos. Admin., Silver Spring, Md., 1994.

Liu, K.-K., Geochemistry of inorganic nitrogen compounds in two marine environments: the Santa Barbara Basin and the ocean off Peru, Ph.D. thesis, Univ. of Calif., Los Angeles, 1979.

Mantoura, R. F. C., C. S. Law, N. J. P. Owens, P. H. Burkill, E. M. S. Woodward, R. J. M. Howland, and C. A. Lewellyn, Nitrogen biogeochemical cycling in the northwestern Indian Ocean, *Deep Sea Res., Part II, 40*, 651–671, 1993.

Marchal, O., P. Monfray, and N. R. Bates, Spring-summer imbalance of dissolved inorganic carbon in the mixed layer of the northwestern Sargasso Sea, *Tellus, Ser. B., 48*, 115–134, 1996.

McElroy, M. B., Marine biological controls on atmospheric CO_2 and climate, *Nature, 302*, 328–329, 1983.

Meybeck, M., Carbon, nitrogen, and phosphorus transport by world rivers, *Am. J. Sci., 282*, 401–450, 1982.

Michaels, A. F., and A. H. Knap, Overview of the U.S. JGOFS Bermuda Atlantic Time-series Study and the Hydrostation S program, *Deep Sea Res., Part II, 43*, 157–198, 1996.

Michaels, A. F., D. A. Siegel, R. J. Johnson, A. H. Knap, and J. N. Galloway, Episodic input of atmospheric nitrogen to the Sargasso Sea: Contributions to new production and phytoplankton blooms, *Global Biogeochem. Cycles, 7*, 339–351, 1993.

Michaels, A. F., N. R. Bates, K. O. Buesseler, C. A. Carlson, and A. H. Knap, Carbon-cycle imbalances in the Sargasso Sea, *Nature, 372*, 537–540, 1994a.

Michaels, A. F., et al., Seasonal patterns of ocean biogeochemistry at the U.S. JGOFS Bermuda Atlantic Time-Series Study site, *Deep Sea Res., Part I, 41*, 1013–1038, 1994b.

Michaels, A. F., D. Olson, J. L. Sarmiento, J. Ammerman, K. Fanning, R. Jahnke, A. H. Knap, R. Lipschultz, and J. Prospero, Inputs, losses and transformations of nitrogen and phosphorus in the pelagic North Atlantic Ocean, *Biogeochemistry*, in press, 1996.

Minas, H., B. Coste, P. LeCorre, M. Minas, and P. Raimbault, Biological and geochemical signatures associated with the water circulation trough the Strait of Gibraltar and in the western Alboran Sea, *J. Geophys. Res., 96*, 8755–8771, 1991.

Minster, J., and M. Boulahdid, Redfield ratios along isopycnal surfaces – A complimentary study, *Deep Sea Res., Part A, 34*, 1981–2003, 1987.

Naqvi, S., S. D. Souza, and C. Reddy, Relationship between nutrients and dissolved oxygen with special reference to water masses in western Bay of Bengal, *Indian J. Mar. Sci., 7*, 15–17, 1978.

Naqvi, S. W. A., Some aspects of the oxygen-deficient conditions and denitrification in the Arabian sea, *J. Mar. Res., 45*, 1049–1072, 1987.

Naqvi, S. W. A., and R. Sen Gupta, 'NO', a useful tool for the estimation of nitrate deficits in the Arabian Sea, *Deep Sea Res., Part A, 32*, 665–674, 1985.

Naqvi, S. W. A., R. J. Noronha, K. Somasundrar, and R. Sen Gupta, Seasonal changes in the denitrification regime of the Arabian Sea, *Deep Sea Res., 37*, 593–611, 1990.

Neftel, A., H. Oeschger, J. Schwander, B. Stauffer, and R. Zumbrunn, Ice core sample measurements give atmospheric CO_2 content during the past 40,000 yr, *Nature, 295*, 220–223, 1982.

Neftel, A., H. Oeschger, T. Staffelbach, and B. Stauffer,

CO_2 record from the Byrd ice core 50,000-5,000 years BP, *Nature, 331*, 609–611, 1988.

Oceanographic Data Facility (ODF), South Atlantic Ventilation Experiment (SAVE), Chemical, physical and CTD data report, Legs 1-3, Scripps Inst. of Oceanogr., La Jolla, Calif., 1992a.

Oceanographic Data Facility (ODF), South Atlantic Ventilation Experiment (SAVE), Chemical, physical and CTD data report, Legs 4-5, Scripps Inst. of Oceanogr., La Jolla, Calif., 1992b.

Orr, J., and J. Sarmiento, Potential of marine macroalgae as a sink for CO_2: Constraints from a 3-D general circulation model of the global ocean, *Water Air Soil Pollut., 64*, 405–421, 1992.

Owens, N. J. P., J. N. Galloway, and R. A. Duce, Episodic atmospheric nitrogen deposition to oligotrophic oceans, *Nature, 357*, 397–399, 1992.

Peng, T.-H., and W. S. Broecker, C/P ratios in marine detritus, *Global Biogeochem. Cycles, 1*, 155–161, 1987.

Physical and Chemical Oceanographic Data Facility (PCODF), Transient tracers in the ocean: North Atlantic study, Shipboard physical and chemical data report, Scripps Inst. of Oceanogr., La Jolla, Calif., 1986a.

Physical and Chemical Oceanographic Data Facility (PCODF), Transient tracers in the ccean: Tropical Atlantic study, Shipboard physical and chemical data report, Scripps Inst. of Oceanogr., La Jolla, Calif., 1986b.

Prather, M., R. Derwent, D. Ehhalt, P. Fraser, E. Sanhueza, and X. Zhou, Other trace gases and atmospheric chemistry, in *Climate Change 94, Radiative Forcing of Climate Change*, pp. 77–126, Intergovt. Panel on Clim. Change, Cambridge, England, 1994.

Redfield, A. C., B. H. Ketchum, and F. A. Richards, The influence of organisms on the composition of sea-water, in *The Sea*, vol. 2, edited by M. N. Hill, pp. 26–77, Wiley-Interscience, New York, 1963.

Roemmich, D., and C. Wunsch, Two trans Atlantic sections: Meridional circulation and heat flux in the subtropical North Atlantic Ocean, *Deep Sea Res., Part A, 32*, 619–665, 1985.

Rueter, J. G., D. A. Hutchins, R. W. Smith, and N. L. Unsworth, Iron nutrition of Trichodesmium, in *Marine Pelagic Cyanobacteria: Trichodesmium and Other Diazotrophs*, edited by E. J. Carpenter, pp. 289–306, Kluwer Acad., Norwell, Mass., 1992.

Sarmiento, J., A tritium box model of the North Atlantic thermocline, *J. Phys. Oceanogr., 13*, 1269–1274, 1983.

Sarmiento, J. L., J. Willebrand, and S. Hellerman, Objective analysis of tritium observations in the Atlantic Ocean during 1971/74. *Tech. Rep. 1*, Princeton Univ., Princeton, N. J., 1982.

Seitzinger, S., and A. Giblin, Estimating denitrification in North Atlantic continental shelf sediments, *Biogeochemistry.*, in press, 1996.

Sen Gupta, R., S. Fondekar, V. Sankaranarayanan, and S. DeSousa, Chemical oceanography of the Arabian Sea, I, Hydrochemical and hydrographic features of the northern basin, *Indian J. Mar. Sci., 4*, 136–140, 1976.

Shaffer, G., A non-linear climate oscillator controlled by biogeochemical cycling in the ocean: An alternative model of Quaternary ice age cycles, *Clim. Dyn., 4*, 127–143, 1990.

Siegenthaler, U., Modeling the dynamics of the global carbon cycle and other natural systems, habilitation thesis, Phys. Inst., Univ. of Bern, Bern, Switzerland, 1982.

Smethie, W. M., Nutrient regeneration and denitrification in low oxygen fjords, *Deep Sea Res., Part A, 34*, 983–1006, 1987.

Smith, S., Phosphorus versus nitrogen limitation in the marine environment, *Limnol. Oceanogr., 29*, 1149–1160, 1984.

Staffelbach, T., B. Stauffer, A. Sigg, and H. Oeschger, CO_2 measurements from polar ice cores: More data from different sites, *Tellus, Ser. B., 43*, 91–96, 1991.

Swift, J., A recent θ-S shift in the deep waters of the northern North Atlantic, in *Climate Processes and Climate Sensitivity, Geophys. Monogr. Ser.*, vol. 29, edited by J. Hansen and T. Takahashi, pp. 39–47, AGU, Washington, D. C., 1984.

Takahashi, T., W. S. Broecker, and S. Langer, Redfield ratio based on chemical data from isopycnal surfaces, *J. Geophys. Res., 90*, 6907–6924, 1985.

Thiele, G., and J. L. Sarmiento, Tracer dating and ocean ventilation, *J. Geophys. Res., 95*, 9377–9391, 1990.

Thomas, W. H., On denitrification in the northeastern tropical Pacific Ocean, *Deep Sea Res., 13*, 1109–1114, 1966.

Tsunogai, S., M. Kusakabe, H. Iizumi, I. Koike, and A. Hattori, Hydrographic features of the deep water of the Bering Sea – The sea of silica, *Deep Sea Res., Part A, 26*, 641–659, 1979.

United Nations Educational, Scientific, and Cultural Organization (UNESCO), Background papers and supporting data on the International Equation of State for Seawater 1980, in *Unesco Technical Papers in Marine Science*, vol. 38, U. N. Educ., Sci., and Cult. Org., Paris, 1981.

Volk, T., and M. I. Hoffert, Ocean carbon pumps: Analysis of relative strengths and efficiencies in ocean-driven atmospheric CO_2 changes, in *The Carbon Cycle and Atmosperic CO_2: Natural Variations Archean to Present, Geophys. Monogr. Ser.*, vol. 32, edited by E. T. Sundquist and W. S. Broecker, pp. 99–110, AGU, Washington, D. C., 1985.

Weiss, R., W. Broecker, H. Craig, and D. Spencer, *Hydrographic Data 1977-1978, GEOSECS Indian Ocean Expedition*, vol. 5, U.S. Govt. Print. Off., Washington, D. C., 1983.

World Ocean Circulation Experiment Hydrographic Programme Special Analysis Centre (WHP SAC), WOCE Atlantic leg A16N: Oceanus 202, electronic form, Hamburg, Germany, 1996a.

World Ocean Circulation Experiment Hydrographic Programme Special Analysis Centre (WHP SAC), Historical cruises: Oceanus 133-7, electronic form, Hamburg, Germany, 1996b.

Wollast, R., The coastal organic carbon cycle: Fluxes, sources and sinks., in *Ocean Margin Processes in Global Change*, edited by R. Mantoura, J.-M. Martin, and R. Wollast, pp. 365–381, John Wiley, New York, 1991.

Wyrtki, K., *Oceanographic Atlas of the International Indian Ocean Expedition (Reprint)*, A. A. Balkema, Rotterdam, Netherlands, 1988.

N. Gruber, Climate and Environmental Physics, Physics Institute, University of Bern, Sidlerstr. 5, 3012 Bern, Switzerland. (e-mail: gruber@climate.unibe.ch)

J. L. Sarmiento, Program in Atmospheric and Oceanic Sciences, Princeton University, Princeton, NJ 08544-0710. (e-mail: jls@splash.princeton.edu)

(Received June 4, 1996; revised December 9, 1996; accepted January 2, 1997.)